AD-A156 952 FATIGUE CRACK PROPAGATION IN MIRAGE IIIO WING MAIN SPAR 1/1
SPECIMENS AND THE..(U) AERONAUTICAL RESEARCH LABS
MELBOURNE (AUSTRALIA) J Y MANN ET AL. JUL 84
UNCLASSIFIED ARL/STRUC-R-405 F/G 20/11 NL

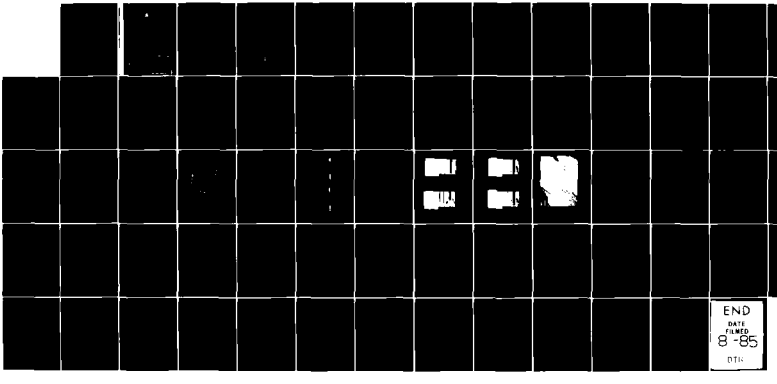

END
DATE FILMED
8-85
DTIC

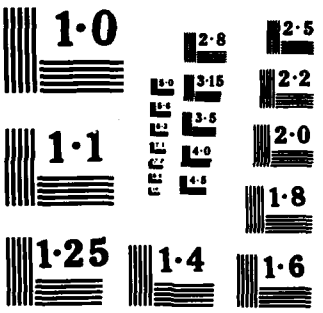
1·0
1·1
1·25
2·8
3·15
3·5
4·0
4·5
1·4
2·5
2·2
2·0
1·8
1·6

ARL-STRUC-R-405

AR-003-937

DEPARTMENT OF DEFENCE

DEFENCE SCIENCE AND TECHNOLOGY ORGANISATION

AERONAUTICAL RESEARCH LABORATORIES

MELBOURNE, VICTORIA

STRUCTURES REPORT 405

FATIGUE CRACK PROPAGATION IN MIRAGE IIIO WING MAIN SPAR SPECIMENS AND THE EFFECTS OF SPECTRUM TRUNCATION ON LIFE

by

J. Y. MANN, R. A. PELL and A. S. MACHIN

APPROVED FOR PUBLIC RELEASE

COPY No

JULY 1984

CONDITIONS OF RELEASE AND DISPOSAL

1. This document is the property of the Australian Government; the information it contains is released for defence purposes only and must not be disseminated beyond the stated distribution without prior approval.
2. The document and the information it contains must be handled in accordance with security regulations applying in the country of lodgement, the following instructions must be observed and dissemination is only with the specific approval of the Releasing Authority as given in the Secondary Distribution statement.
3. This information may be subject to privately owned rights.
4. The officer in possession of this document is responsible for its safekeeping. When no longer required this document should NOT BE DESTROYED but returned to

   Defence Information Services Branch, Campbell Park, Canberra, ACT 2600 Australia.

AR-003-937

DEPARTMENT OF DEFENCE
DEFENCE SCIENCE AND TECHNOLOGY ORGANISATION
AERONAUTICAL RESEARCH LABORATORIES

STRUCTURES REPORT 405

FATIGUE CRACK PROPAGATION IN MIRAGE IIIO WING MAIN SPAR SPECIMENS AND THE EFFECTS OF SPECTRUM TRUNCATION ON LIFE

by

J. Y. MANN, R. A. PELL and A. S. MACHIN

SUMMARY

As part of an investigation into the life extension and safe operation of the wings of the Mirage IIIO aircraft, a fatigue testing program and extensive fractographic examination was undertaken on specimens representing the critical section of the spar to assess the effects of truncating the maximum positive loads of the spectrum and provide information relating to fatigue crack propagation rates.

Under the fighter-type load spectrum adopted, truncation of the maximum load from +7·5 g to +6·5 g or to +5 g did not result in an increase in fatigue life, presumably because of the loss of the crack retardation potential of this rarely occurring high positive load.

A good linear relationship was found between the log. life and log. crack depth for individual specimens. At the smallest crack depth used for analysis (0·3 mm) no significant differences were found between the standard deviations of log. life to crack "initiation", for propagation or to final failure, nor in the corresponding standard deviations of arithmetic lives.

In considering the more general question of whether the greater contribution to variability in total life comes from that in "initiation" life or that in "propagation" life, cognizance must be taken of the analytical basis of the assessment—whether arithmetic or logarithmic. On a logarithmic basis the standard deviation of life to the formation of a crack of specific depth decreases with increasing crack depth, whereas on an arithmetic basis it increases. The converse applies in each case for the variability in propagation lives. On an arithmetic basis the standard deviation of the crack propagation rate increases with crack depth, that at a depth of 5 mm being about seven times that at a depth of 0·5 mm. However the standard deviation of log. crack propagation rate is substantially constant irrespective of crack depth.

These findings are of significance in the numerical implementation of safe-life, durability and damage tolerance fatigue philosophies.

POSTAL ADDRESS: Director, Aeronautical Research Laboratories,
Box 4331, P.O., Melbourne, Victoria, 3001, Australia

CONTENTS

	Page No.
1. INTRODUCTION	1
2. TESTING PROGRAM	1
2.1 Material and Test Specimens	1
2.2 Flight-by-Flight Loading Sequences	2
2.3 Fatigue Tests and Results	2
2.4 Crack Propagation Measurements	3
3. DISCUSSION	4
3.1 Lives to Failure	4
3.2 Crack Propagation Data	4
4. CONCLUSIONS	7
ACKNOWLEDGEMENTS	7
REFERENCES	
APPENDIX—Fractographic crack growth measurements	
TABLES	
FIGURES	
DISTRIBUTION LIST	
DOCUMENT CONTROL DATA	

1. INTRODUCTION

An extensive fatigue testing program undertaken at the Aeronautical Research Laboratories (ARL) investigated potential methods for increasing the fatigue life of the wing main spar of the Mirage IIIO fighter operated by the Royal Australian Air Force (RAAF). This research, which has been reported in References 1 to 3, led to the adoption of interference-fit steel bushes at bolt holes as a means for providing the required extension in life.

A basic criterion of the life-extension procedures was that existing fatigue cracks should be completely removed. However, the variability in the size of fatigue cracks which developed throughout the Mirage fleet at critical bolt holes in the spar lower flange was such as to preclude some spars from being effectively refurbished by the installation of bushes. Furthermore, because of the large fatigue cracks which had developed in the spars of some aircraft, consideration was given to imposing flight loading limits for particular aircraft to reduce the risk of in-flight structural failure—in effect, to truncate the maximum positive load levels in the loading spectrum.

In view of the findings (Refs 4–6) that the omission or truncation of rarely-occurring high loads can result in lower fatigue lives by reducing crack retardation effects, a series of fatigue tests was undertaken to explore the implications of truncating the maximum positive load levels of the previously used loading spectrum. The results of this investigation, together with those of constant-amplitude tests to provide basic information for life-estimation purposes, are presented in this report. Fractographic crack propagation studies also provided a considerable amount of information on variations in fatigue crack initiation and propagation lives and in crack propagation rates.

2. TESTING PROGRAM

2.1 Material and Test Specimens

The wing main spar of the Mirage III is a large forging in aluminium alloy to the French Specification A-U4SG (equivalent to the American alloy 2014 covered by Specification QQ-A-255a). For this investigation four batches of A7-U4SG aluminium alloy plate (equivalent to a later version of 2014—namely 2214) of thickness between 46 and 55 mm were used for the manufacture of fatigue specimens. These were given the ARL serial coding GK, GN, GT and GZ.

Fatigue test specimens (Fig. 1) were designed to represent the spar flange at the critical inboard section.* The specimens were oriented with their longitudinal axes parallel to the rolling direction of the plate. Details of the cutting plans are given in Reference 3. Because of production differences between Mirage III wings manufactured in Australia and overseas the detail at the Single Leg Anchor Nut (SLAN) incorporated three different rivet systems for attaching the nut to the specimen.

* The 8 mm and 10 mm bolts connecting the skin plate to the "spar" section were torqued to 7·9 and 19·2 Nm respectively.

(i) 2·5 mm diameter countersunk-head A-U4G aluminium alloy rivets† inserted from the skin plate surface of the spar and with their tails peened against the cage of the nut;

(ii) 3·0 mm diameter countersunk-head A-U4G rivets† installed as for (i); and

(iii) 0·125 inch diameter universal head 2117 aluminium alloy rivets inserted from the "inner" surface of the spar flange, i.e. with their heads against the leg of the anchor nut and tails peened into the countersunks at the skin plate surface of the flange. This was the SLAN rivet arrangement in Australian-made wings. About 75% of the specimens used in this investigation were of this type.

Overall, the investigation involved the fatigue testing of 68 specimens. Tensile test specimens and compact tension fracture toughness specimens were manufactured from a sample of broken fatigue specimens of each plate. The results of these tests, together with the chemical compositions of the plates, are given in Table 1.

2.2 Flight-by-Flight Loading Sequences

The basic fatigue load spectrum adopted for this investigation (Type 1—Fig. 2) was a simplified version of that used for the full-scale fatigue test on a Mirage III structure at the F+W Emmen, Switzerland. It was transformed into a 100-flight load sequence consisting of four different flight types (A^1, A, B and C) as illustrated in Fig. 3. Cycles of +6·5 g/−1·5 g and +7·5 g/−2·5 g (a total of 39 cycles in 100 flights) were applied at a cyclic frequency of 1 Hz, whereas the remaining 1950 cycles per 100 flights were at 3 Hz. Table 2 gives the total numbers of cycles of each load range in a 100-flight sequence.

The first modification to the load spectrum was to reduce the severity of the negative part so that it corresponded more closely to the then current usage pattern of RAAF Mirage IIIO aircraft. This modification (designated the Type II spectrum and characterized in Fig. 2 and Table 2) was not expected to provide any significant increase in life (Refs 6–8). Types III and IV spectra retained the negative part of the Type II spectrum but truncated the maximum positive load to +6·5 g and +5 g respectively. Details are given in Fig. 2 and Table 2.

2.3 Fatigue Tests and Results

All fatigue tests were carried out in a Tinius-Olsen servo-controlled electro-hydraulic fatigue machine, using sine wave loading. Loads on the test specimen were based on the assumption that +7·5 g corresponded to a *gross area* stress (not including the skin plate) of 180 MPa at the SLAN section and that there was a linear stress/g relationship, i.e. the 1 g gross area stress was 24 MPa. At 7·5 g the testing machine load was nominally 404 kN.

Constant-amplitude fatigue tests were made at each of the five cyclic load ranges which formed the basis for the Type I loading sequence, i.e. +7·5 to −2·5 g, +6·5 to −1·5 g, +5 to 0 g, +4 to +0·5 g and +3 to +1 g. For each range the cyclic frequency was the same as for the flight-by-flight tests. These tests involved 17 specimens incorporating 2117 aluminium alloy SLAN rivets. The test results are listed individually in Table 3, and plotted on the S–N diagram—Fig. 4. A second order polynomial expression was fitted to the data to derive the average S–N curve.

The 100-flight flight-by-flight load sequence was achieved using an EMR Model 1641 programmable function generator controlled by a punched tape. Fatigue tests under the basic spectrum (Type I) were performed using specimens of each of the three SLAN rivet systems and involved six, eleven and fourteen specimens with 2·5 mm A-U4G, 3·0 mm A-U4G and 0·125 inch 2117 rivets respectively. The results of these tests are listed in Table 4. However, *all* of the tests involving Spectra Types II, III and IV were performed using specimens with 2117 SLAN rivets.

† The A-U4G rivets were inserted in the solution-treated condition. Specimens incorporating such rivets were not fatigue tested until at least four days after rivet insertion to allow full precipitation hardening to occur.

Firstly, fatigue tests to complete fracture were carried out under each of these three spectra (four specimens in each case). These were followed by partial fatigue testing under Spectrum Type II until the development of cracks of nominated lengths in the bore of hole (1), after which specimens were fatigue tested to fracture under either Spectra Types III or IV.* Fatigue tests under Spectra Types II, III and IV involved a total of 20 specimens. The results are listed in Table 5.

2.4 Crack Propagation Measurements

Macrophotographs of the fracture surfaces of specimens taken from each of the four batches of material are shown in Fig. 5. The fatigue fractures developed from multiple origins, predominantly at the bore of the bolt hole closest to the rear face of the specimens and nearer to the "skin plate" end of the hole. In their early stages the individual cracks were essentially semi-circular but they coalesced with fatigue cycling to form a common crack front the shape of which is typified by the photographs in Fig. 5.

The identification of the regular fractographic markings associated with the once-per-hundred-flights $+7{\cdot}5$ g load and the adjoining $+6{\cdot}5$ g loads in the Types I and II spectra enabled this feature of the fracture surface (Fig. 6) to be used to measure cracks which developed from the rear side of the 8 mm SLAN bolt hole. Unfortunately, the absence of such a feature on the fracture surfaces of specimens tested under the spectra with positive load truncation (Types III and IV) negated attempts to measure crack growth in these cases and determine whether the change in spectrum significantly altered fatigue crack initiation lives and crack propagation rates. However, by fractographic examination it was possible, in some cases, to measure the maximum crack depth at which the transition from Spectrum II to Spectrum III or IV had occurred. For specimen GZ2A4 (Type II to Type III) it was $1{\cdot}02$ mm, while for the four specimens involving Type II to Type IV they were $3{\cdot}54$ mm (GT1L), $0{\cdot}81$ mm (GZ2A9), $2{\cdot}27$ mm (GZ2B7) and $2{\cdot}12$ mm (GZ2C10).

For about half the specimens incorporating $2{\cdot}5$ mm and $3{\cdot}0$ mm A-U4G SLAN rivets (which were tested under the Type I spectrum only) crack growth was determined using $\times 25$ magnification macrophotographs of the fracture surfaces, supplemented by observations of the fracture surfaces (at higher magnification) using an optical microscope. Crack growth measurements were made in a direction approximately perpendicular to the bore of the hole towards the side of the specimens. In four cases the smallest measureable crack depth was less than about $0{\cdot}3$ mm, while the greatest minimum depth was $2{\cdot}15$ mm. Figures 7 and 8 show the crack growth characteristics of some of the specimens incorporating $2{\cdot}5$ mm and 3 mm SLAN rivets.

A much more extensive fractographic study was made of the 13 specimens incorporating $0{\cdot}125$ inch SLAN rivets which were tested under the Type I spectrum. This included the use of macrophotographs, an optical stereo microscope and a metallographic microscope. Details of the techniques employed are given in Appendix 1. In two cases (specimens GZ3A10 and GK1E10) crack growth measurements were obtained at distances of less than $0{\cdot}1$ mm from the hole and in ten cases at less than $0{\cdot}3$ mm. The incremental crack growth data obtained using the three techniques was combined to provide the series of plots of fatigue life versus crack depth illustrated in Fig. 9(*a*).

Crack growth data for three specimens tested under Spectrum II are shown in Fig. 10. In these cases the minimum crack depths at which measurements could be taken were $0{\cdot}07$, $0{\cdot}14$ and $0{\cdot}22$ mm respectively.

---

* Specimens subsequently tested under Spectrum IV had larger cracks than those subsequently tested under Spectrum III.

3. DISCUSSION

3.1 Lives to Failure

Table 6 summarizes the fatigue test results under the four loading spectra. The general pattern of a greater indicated mean life for Spectrum II compared with Spectrum I (because of a reduction in the overall fatigue range), and a reduced mean life under Spectra III and IV compared with Spectrum II (because of a removal of potential crack retardation effects associated with the $+7{\cdot}5$ g load) is what might have been expected. However, statistical comparisons of the average fatigue lives to failure (based on a level of significance of 5%) for specimens incorporating 0·125 inch SLAN rivets indicate that there are *no significant differences* between the lives under Spectra I and II (lines (3) and (4)), between II and III (lines (4) and (5)), between II and IV (lines (4) and (6)) and between III and IV (lines (5) and (6)). The total lives to failure of specimens pre-cracked under Spectrum II and then tested to failure under either Spectra III or IV (lines (7*a*) and (8*a*)) are also not significantly different to that under Spectrum II alone (line (5)). It should be noted however that, except for the tests under Spectrum I, the sample size in each case was relatively small (three or four specimens) and that the significance of differences in the mean lives is sensitive to the numerical values of the standard deviations in life of the respective samples. Thus, on this experimental evidence, the strongest conclusion is that truncation of the maximum positive load to either $+6{\cdot}5$ g or $+5$ g provides *no increase* in life compared with that under the untruncated spectrum.

Estimates of the lives to failure (based on the simple Miner linear cumulative damage hypothesis) under the various spectra are given in Table 7. Although this approach might provide a useful method for estimating the lives under the untruncated positive load spectra actually used, it clearly overestimates the lives under the truncated spectra, presumably because it does not compensate for the potential loss of the crack retardation effects associated with the $+7{\cdot}5$ g loads.

3.2 Crack Propagation Data

The individual data points in Fig. 9(*a*) for specimens incorporating 0·125 inch SLAN rivets which were tested under the Type I Spectrum formed the basis for the curves shown in Fig. 9(*b*). These were constructed by joining adjacent data points with straight lines. A comparison of the crack growth data for these specimens and those incorporating 2·5 mm or 3 mm SLAN rivets (Figs 7(*b*) and 8(*b*)) indicates very little overall difference in the general crack propagation behaviour of the three types of specimen. The crack growth characteristics of specimens tested under Spectrum II are similar to those tested under Spectrum I except perhaps for cracks of less than about 1 mm in depth. It is clear, however, that the individual specimens exhibit marked differences in crack growth characteristics at small crack depths. Because of the lack of experimental evidence relating to the development of cracks up to the minimum sizes indicated in Figs 7 to 10, in no case was any attempt made to extrapolate the curves back to zero crack depth.

A further analysis of the basic data for specimens tested under Spectrum I was made to explore possible relationships between flights and crack depth, i.e. linear/log. and log./log. The first relationship was that assumed by Grandage and Sparrow (Ref. 9) for their interpretation of fatigue cracking in the wing main spars of RAAF Mirage aircraft, while the second had been used in the preliminary analysis of some of the current data. Figure 9(*c*) shows the curves for the 0·125 inch SLAN rivet specimens using linear/log. coordinates; while Figs 7(*c*), 8(*c*) and 9(*d*) show the curves for the 2·5 mm, 3·0 mm and 0·125 inch rivet specimens respectively using log./log. coordinates. Figures 11(*a*) to 11(*d*) group the data for the 0·125 inch SLAN rivet specimens from Fig. 9(*d*) according to the four batches of material. These curves do not indicate a strong linear correlation between life and log. crack depth, but the data for the 13 individual specimens (Table 8) indicate a very good linear correlation between log. life and log. crack depth

in every case. However, when all the 1` sets of data are pooled the overall goodness of fit for a single straight line relationship deteriorates considerably. Figures 7(*b*), 8(*b*) and 9(*b*) also show the crack growth curve (taken from Reference 10) for a Mirage spar which failed during a full-scale fatigue test at the F+W, Emmen, Switzerland using a loading spectrum similar to Spectrum I These data are in good agreement with the results of the present investigation.

The correct interpretation of variability in fatigue parameters is essential in the implementation of safe-life, durability and damage tolerance fatigue philosophies; and the information available from this investigation—particularly that obtained from specimens tested under Spectrum I—provides a comprehensive set of relevant data on fatigue crack behaviour in thick sections. Also of importance (from a more general viewpoint) is that the specimens were taken from several different batches of material—a situation which would occur in the manufacture of a fleet of aircraft.

Specimens incorporating 0·125 inch SLAN rivets furnished the largest sample on which detailed crack propagation data were obtained. Analyses of these data were made on the basis of the variability in crack depths at specified lives, and the variability in lives at specified crack depths.

Crack depth data at lives of 3742, 4442, 5342, 6242 and 7142 flights were plotted on both linear and logarithmic probability paper and are shown in Fig. 12. These lives covered the range from no failures to that by which two specimens had failed. As the logarithmic relationship for crack depth provided a better fit for the data (and furthermore the arithmetic analysis indicated crack depths of less than zero at -1 standard deviation) a more detailed analysis of the data was made on a "logarithmic" basis and the results are summarized in Table 9. The numerical values (particularly those for 3742 flights which was prior to the first complete failure) provide some indication of the variability in crack depth which could be expected for cracking from fastener holes in a heavy section when multiple fatigue crack initiation was involved.

The view has been expressed (see for example Reference 11) that the crack initiation phase is the major contributor to scatter in total fatigue lives and that, under nominally identical fatigue testing conditions, there is relatively much smaller scatter in crack propagation lives. However, an analysis of experimental data made by Mann (Ref. 12) indicated that the standard deviations of log. life for crack initiation, crack propagation and total failure may not be significantly different. It is usually possible to accurately measure the life to total failure, but there are practical problems in precisely identifying fatigue crack initiation—and hence crack initiation lives and crack propagation lives and their variabilities. Fatigue crack "initiation" is frequently regarded as that life corresponding to a measurable crack of less than 1 mm.

To study the variability in fatigue lives associated with the development of cracks of different depths, linear interpolations of lives were made between those corresponding to the nearest larger and smaller crack depths selected for analysis. The lives corresponding to nominated crack depths of from 0·1 mm to 5·5 mm are given in Table 10, together with the remaining life of each specimen after the development of cracks of these depths. However, in order to provide a coherent set of information covering crack depths of from 0·3 mm to 5·5 mm only those data for the first ten specimens listed in Table 10 were used in the subsequent analysis. For these specimens the "initiation" life (0·3 mm deep crack) as a portion of total life was from 26% to 48%, and the general correlation between initiation (as a portion of the total life) and the total life was poor. The analysis which follows was done on the basis of both log. normal and normal distributions of life.

Table 11 gives the average lives to the development of cracks of different depths and the propagation lives to failure from the specified depths (and their respective standard deviations), and the lives in each case corresponding to ± 1 standard deviation from the average. The data are summarized in Figs 13 and 14. Trends similar to those indicated in Figs 13 and 14(*a*) have been reported by Jost and Esson (Ref. 13) for D6ac steel.

In terms of numerical values of lives (whether average or those corresponding to ± 1 standard deviation), there is little difference whether the data be analyzed on a logarithmic or arithmetic basis. However, the basis for the analysis becomes an important consideration when attempting to resolve the question of which phase of the fatigue process (crack initiation or crack propagation)

contributes most to scatter in total life. At the smallest crack depth of 0·3 mm there are no significant differences in the standard deviations of log. life for "initiation", propagation and final failure, or for the corresponding standard deviations of arithmetic lives. Referring to Figs 13 and 14 there are no significant differences in the standard deviations of lives to develop cracks of depths from between 0·3 and 5·5 mm irrespective of whether the analyses be based on logarithmic or arithmetic values. Although there are no significant differences in the standard deviations of lives for crack propagation for crack depths from 0·3 mm up to 3·0 mm (irrespective of the basis for the analysis), the differences (compared with the value at 0·3 mm) do become significant for crack depths of 3·5 mm and greater. Similarly, there are no significant differences between the standard deviations of lives to initiate a crack of 0·3 mm and those to develop it to failure for crack depths of up to 2·0 mm. The differences become significant (on an arithmetic basis) at 2·5 mm and at 4 mm on a logarithmic basis.

However, Figs 14 (*a*) and 14 (*b*) indicate that, depending on the basis of the analysis, two completely different conclusions could be arrived at for the changes in variability between the lives to the "initiation" and those for the "propagation" of cracks from a specified depth, e.g. for propagation the standard deviation of log. life increases with crack depth whereas the arithmetic standard deviation decreases. Furthermore, at crack depths of less than 0·3 mm (i.e. extrapolating back to a true "initiation") the trends of the data reproduced in Fig. 14(*a*) suggest that the s.d. of log. life to initiation may be significantly greater than that for propagation, whereas from the arithmetic analysis (Fig. 14(*b*)) the reverse appears to be the case. This finding should be recognized in the assessment of the contribution to the variability in total life made by the two major phases of the fatigue process. Thus, from the viewpoint of the life to propagate a crack from a small nominated depth—for example 0·5 mm (0·020 inch) or 1·25 mm (0·050 inch) which have particular significance in fail-safe and damage tolerance analysis—the assignment of a "safety factor" on crack propagation life could be markedly dependent on both the base used for the analyses of variability and the nominated initial crack size.

The fractographic data also allowed the determination of crack growth rates at nominated crack depths. These were derived from the data for the measured crack growth increments at measured crack depths. Third order polynomial curves were fitted to the data for each individual specimen and used to determine the fatigue crack growth rates at selected crack depths, the average crack growth rates being shown in Fig. 15(*a*) and the variability in growth rate in Fig. 15(*b*). Because of the influence of edge effects, the uncertainties in being able to identify and accurately measure the boundaries of the fracture markings at very large crack depths (corresponding in most cases to the last few hundred flights before failure), and the potential interactions of cracks developing on the other side of the hole, the analysis of crack growth rates was limited to a maximum crack depth of about 5·0 mm. As before, the analysis was confined to the first 10 specimens in Table 10.

Figure 15(*a*) shows that the crack growth rate increases with increasing crack depth. The relationship between these two variables can be described by a power function of the form $y = ax^b + c$.* From Fig. 15(*b*) it may be seen that, on an arithmetic basis, the variability in crack growth rate increases with increasing crack depth. Compared with the standard deviation of crack growth rate at 0·5 mm crack depth the standard deviations are significantly greater for cracks having depths of 1·5 mm and more. However, on a logarithmic basis the variability in crack growth rate is substantially constant, irrespective of crack depth. This follows from the properties of a power function.* It is uncertain whether the inflections in the two curves shown in Fig. 15(*b*) at small crack depths are a real effect or simply associated with limitations in the accuracy with which fractographic measurements could be made at such small crack depths.

---

* If '*a*' is the random variable and '*b*' and '*c*' are constants then this equation may be transformed to:

$$(y-c) = ax^b$$

and

$$\log (y-c) = \log a + b \log x.$$

4. CONCLUSIONS

1. Under the load spectrum adopted for this investigation truncation of the maximum load from +7·5 g to +6·5 g or to +5 g did not result in an increase in fatigue life, presumably because of the loss of the crack retardation potential of this rarely occurring high positive load.

2. A good linear relationship was found between life and crack depth for individual specimens when using log.–log. coordinates.

3. At the smallest crack depth used for analysis (0·3 mm) there are no significant differences in the standard deviations of log. life to crack "initiation", for propagation and to final failure, nor in the corresponding standard deviations of arithmetic lives.

4. In considering the general question of whether the greater contribution to variability in total life comes from that in "initiation" life or that in "propagation" life, cognizance must be taken of the analytical basis for the assessment—whether arithmetic or logarithmic.

5. On a logarithmic basis the standard deviation of life to crack "initiation" *decreases* with increasing crack depth, whereas on an arithmetic basis it *increases*. The converse applies in each case for the variability in propagation lives.

6. On an arithmetic basis the standard deviation of the crack propagation rate increases with crack depth, that at a depth of 5 mm being about seven times that at a depth of 0·5 mm. However the standard deviation of the log. crack propagation rate is substantially constant irrespective of crack depth.

7. The above findings are of significance in the numerical implementation of safe-life, durability and damage tolerance fatigue philosophies.

ACKNOWLEDGEMENTS

The authors express their appreciation to Mr W. F. Lupson of Structures Division for his assistance, in particular his attention to detail during the preparation of the fatigue test specimens.

REFERENCES

1. Mann, J. Y., Revill, G. W., and Lupson, W. F. Improving the fatigue performance of thick aluminium alloy bolted joints by hole cold-expansion and the use of interference-fit steel bushes. *Dept. Defence Aeronaut. Res. Labs.* Structures Note 486, April 1983.

2. Mann, J. Y., Machin, A. S., Lupson, W. F., and Pell, R. A. The use of interference-fit bolts or bushes and hole cold-expansion for increasing the fatigue life of thick-section aluminium alloy bolted joints. *Dept. Defence Aeronaut. Res. Labs.* Structures Note 490, August 1983.

3. Mann, J. Y., Machin, A. S., and Lupson, W. F. Improving the fatigue life of the Mirage IIIO wing main spar. *Dept. Defence Aeronaut. Res. Labs.* Structures Report 398, January 1984.

4. Schijve, J., Jacobs, F. A., and Tromp, P. J. Crack propagation in aluminium alloy sheet materials under flight simulation loading. *Natl Lucht-en Ruimtevaartlab.* TR-68117U, December 1968.

5. Jarfall, L. Influence of variations of a manoeuvre load spectrum. *Problems with fatigue in aircraft. Proceedings of 8th ICAF Symposium*, Emmen, F+W, 1975, pp. 3.7/1–3.7/12.

6. Darts, J. The influence of the largest and smallest loads in an aircraft spectrum on the fatigue endurance of a bolted joint. *Royal Aircr. Establ.* Tech. Rep. 77138, September 1977.

7. Hsu, T. M., and McGee, W. M. Effects of compressive loads on spectrum fatigue crack growth rate. *Effect of load spectrum variables on fatigue crack initiation and propagation.* ASTM STP No. 714, October 1980, pp. 80–90.

8. Magnusson, A. Comparison of different fighter load spectra. *Flygtekn. Försöksanst.* TN 1982-02, 25 March 1982.

9. Grandage, J. M., and Sparrow, J. G. Analysis and interpretation of cracks in the RAAF Mirage fleet. *Dept. Defence Aeronaut. Res. Labs.* Structures Note 476, July 1981.

10. Goldsmith, N. T. Fractographic examinations relevant to the F+W Mirage fatigue test. *Dept. Defence Aeronaut. Res. Labs.* Materials Tech. Memo. 371, August 1978.

11. Kirkby, W. T., Forsyth, P. J. E., and Maxwell, R. D. J. Design against fatigue—current trends. *Aeronaut. Jnl*, Vol. 84, No. 829, January 1980, pp. 1–12.

12. Mann, J. Y. Scatter in fatigue life—a materials, testing and design problem. *Materials, experimentation and design in fatigue.* (Editors: F. Sherratt and J. B. Sturgeon). Guildford, IPC Business Press, 1981, pp. 390–423.

13. Jost, G. S., and Esson, G. P. Fatigue of D6ac steel specimens—means and variabilities under programmed loading. *Dept. Supply Aeronaut. Res. Labs.* Structures and Materials Report 349, April 1974.

TABLE 10

Flights to Reach Nominated Crack Depths

Specimen No.	GZ3A10	GK1E10	GN3B	GN4B	GK1B7	GN1D	GT2G	GZ2C12	GZ3C8	GT10	GT3F	GK1D9	GZ2A5
Crack depth (mm)	Flights (N_n) to given crack depth and then to failure ( )												
0·1	3812	3135	—	—	—	—	—	—	—	—	—	—	—
	(8049)	(5407)	—	—	—	—	—	—	—	—	—	—	—
0·2	4068	3668	2828	2004	—	—	—	—	—	—	—	—	—
	(7793)	(4874)	(5714)	(5738)	—	—	—	—	—	—	—	—	—
0·3	4369	4068	3047	2339	3519	2628	2747	1828	2563	4439	—	—	—
	(7492)	(4474)	(5495)	(5403)	(5843)	(6414)	(4901)	(5112)	(5760)	(4801)	—	—	—
0·4	4682	4346	3280	2586	3954	2840	2982	2021	2956	4764	3646	3869	—
	(7179)	(4196)	(5262)	(5156)	(5408)	(6202)	(4666)	(4919)	(5367)	(4476)	(3996)	(4773)	—
0·5	5005	4563	3505	2793	4312	2993	3196	2198	3244	5013	3981	4150	—
	(6856)	(3979)	(5037)	(4949)	(5050)	(6049)	(4452)	(4742)	(5079)	(4227)	(3661)	(4492)	—
1·0	6178	5467	4481	3582	5674	3918	4042	3029	4250	5881	5075	5139	—
	(5683)	(3075)	(4061)	(4160)	(3688)	(5124)	(3606)	(3911)	(4073)	(3359)	(2567)	(3503)	—
1·5	7120	6059	5312	4231	6634	4799	4641	3707	4990	6528	5627	5785	—
	(4741)	(2483)	(3230)	(3511)	(2728)	(4243)	(3007)	(3233)	(3333)	(2712)	(2015)	(2857)	—

TABLE 9

Summary of Crack Depth Data at Specified Flights

Specimen number	Crack depth (mm) at flight number				
	3742	4442	5342	6242	7142
GZ2C12	1·530	2·076	3·312	6·028	—
GN4B	1·106	1·670	2·563	3·744	6·117
GZ2A5	4·527	—		Specimen failed	
GN1D	0·880	1·313	1·876	2·804	3·845
GZ3C8	0·722	1·116	1·808	2·703	4·310
GT2G	0·820	1·320	2·164	3·433	5·758
GN3B	0·624	0·979	1·520	2·210	3·273
GK1E10	0·217	0·450	0·921	1·690	3·011
GK1B7	0·347	0·540	0·850	1·262	1·809
GT3F	0·427	0·680	1·188	2·253	4·472
GZ3A10	0·074	0·324	0·643	1·030	1·515
GK1D9	0·364	0·608	1·140	2·007	3·578
GT10	<0·301	0·301	0·667	1·264	2·324
Log. of average depth	−0·222	−0·099	0·136	0·351	0·524
Average depth (mm)	0·600	0·796	1·368	2·244	3·345
s.d. of log. depth	0·448	0·276	0·230	0·222	0·193
Depth at −1 s.d. (mm)	0·214	0·421	0·805	1·347	2·143
Depth at +1 s.d. (mm)	1·681	1·504	2·326	3·738	5·220

TABLE 8

Relationships Between Crack Depths and Lives

log. (Crack depth) = A+B log. (Flights)

Specimen number	A	B	r^2
GZ3A10	−12·3357	+3·2404	0·977
GK1E10	−15·3178	+4·0995	0·999
GN3B	−10·3276	+2·8196	0·990
GN4B	−9·1624	+2·5701	0·998
GK1B7	−10·4016	+2·7757	0·989
GN1D	−8·8061	+2·4402	0·994
GT2G	−10·6309	+2·9454	0·998
GZ2C12	−7·7882	+2·2330	0·993
GZ3C8	−9·6092	+2·6512	0·998
GT10	−16·5443	+4·3896	0·999
GT3F	−13·1463	+3·5640	0·981
GK1D9	−13·7220	+3·7023	0·995
GZ2A5	−7·1201	+2·1765	0·996
13 Pooled	−7·0233	+1·9315	0·560
99% Confidence Interval: Lower limit	−7·6703	+1·7576	
99% Confidence Interval: Upper limit	−6·3763	+2·1054	

TABLE 7

Estimated Lives Under Different Spectra

Load range (g)	Cycles to failure (N)	Cycles and (damage) per 100 flights in Spectra Types I, II, III and IV			
		I	II	III	IV
10	4 173	1 (0·000240)	—	—	—
9·9	4 257	—	1 (0·000235)	—	—
8	7 858	38 (0·004836)	—	—	—
6·85	14 185	—	38 (0·002679)	39 (0·002749)	—
5	51 940	400 (0·007701)	—	—	—
4·45	82 981	—	400 (0·004820)	400 (0·004820)	439 (0·005290)
3·5	203 798	450 (0·002208)	—	—	—
3·25	263 057	—	450 (0·001711)	450 (0·001711)	450 (0·001711)
2	1 059 986	1100 (0·001038)	1100 (0·001038)	1100 (0·001038)	1100 (0·001038)
Total damage per 100 flights		0·016023	0·010483	0·010318	0·008039
Estimated life (flights)		6241	9540	9692	12 440
Actual life (flights)		8213	10 353	7612	7665
Ratio Actual/Estimated		1·32	1·09	0·79	0·62

TABLE 6

Summary of Fatigue Test Results

	Table	SLAN rivets	Spectrum type	Test	Number in sample	Log. average life (flights)	s.d. log. life	Life ratio
(1)	4(*a*)	2·5 mm	I	Control	6	7309	0·055	
(2)	4(*b*)	3 mm	I	Control	11	6852	0·117	
(3)	4(*c*)	0·125 inch	I	Control	*13	8213	0·085	
(4)	5(*a*)	0·125 inch	II	Negative spectrum changed	*3	9471	0·047	(4)/(3) = 1·15
(5)	5(*b*)	0·125 inch	III	Positive spectrum trunc. +6·5 g	*3	7092	0·069	(5)/(4) = 0·75
(6)	5(*c*)	0·125 inch	IV	Positive spectrum trunc. +5 g	*3	7945	0·011	(6)/(4) = 0·84
(7*a*)	5(*d*)	0·125 inch	II/III	Total life	4	9832	0·130	(7*a*)/(4) = 1·04
(7*b*)	5(*d*)	0·125 inch	II/III	After truncation	4	4774	0·209	
(8*a*)	5(*e*)	0·125 inch	II/IV	Total life	4	7535	0·085	(8*a*)/(4) = 0·80
(8*b*)	5(*e*)	0·125 inch	II/IV	After truncation	4	2555	0·130	

* For specimens which failed through SLAN section.

TABLE 5(e)

Specimens Cracked Under Spectrum Type II, Then Type IV to Failure

Specimen number	Flights under Type II spectrum	Crack length (mm)	Flights under Type IV spectrum	Total flights to failure	Failing load (kN)	Failure details
GT1L	5400	9·5	2142	7542	271	Large crack rear side hole (1). Crack forward side hole (1). Small cracks both sides of holes (2) and (3)
GZ2A9	6000	10·5	3931	9931	271	Large cracks both sides hole (1). Small cracks both sides of holes (2) and (3)
GZ2B7	4100	11	2475	6575	271	Same as GZ2A9
GZ2C10	4500	11	2046	6546	271	Same as GZ2A9

TABLE 5(c)

Spectrum Type IV: Negative Severity Reduced, Positive Truncated to +5 g

Specimen number	Flights to failure	Failing load (kN)	Failure details
GN30	6883	269	Failed through hole (8)*
GT1P	7715	263	Large cracks both sides hole (1). Minor cracking holes (2) and (3)
GZ3A8	8042	269	Large crack rear side hole (1). Crack forward side hole (1)
GZ2D10	8083	269	Large crack rear side hole (1). Crack forward side hole (1). Small cracks both sides of holes (2) and (3)

* Not used in any statistical comparisons of fatigue lives because of failure locations

TABLE 5(d)

Specimens Cracked Under Spectrum Type II. Then Type III to Failure

Specimen number	Flights under Type II spectrum	Crack length (mm)	Flights under Type III spectrum	Total flights to failure	Failing load (kN)	Failure details
GT1D	6000	7	6242	12 242	325	Large cracks both sides hole (1). Small cracks forward of holes (2) and (3)
GZ2B3	5000	6	6115	11 115	323	Large crack rear side hole (1). Crack forward side hole (1). Small cracks both sides of holes (2) and (3)
GZ2C2	5000	6	5870	10 870	329	Large cracks both sides hole (1). Cracks forward sides of holes (2) and (3)
GZ2A4	4000	7·5	2319	6 319	325	Cracks both sides hole (1). Small cracks both sides holes (2) and (3)

TABLE 5(a)

Spectrum Type II: Negative Severity Reduced

Specimen number	Flights to failure	Failing load (kN)	Failure details
GN3G	13 523	337	Failed through hole (8)*
GT1F	9346	337	Large cracks both sides of hole (1)
GZ3C6	10 615	345	Large crack rear side hole (1). Crack forward side hole (1). Small cracks both sides of holes (2) and (3)
GZ2D1	8562	325	Same as GZ3C6

* Not used in any statistical comparisons of fatigue lives because of failure location.

TABLE 5(b)

Spectrum Type III: Negative Severity Reduced, Positive Truncated to +6·5 g

Specimen number	Flights to failure	Failing load (kN)	Failure details
GN3P	9415	344	Failed through hole (8)*
GT1B	6175	318	Large cracks both sides hole (1). Minor cracking holes (2) and (3)
GZ3C3	8442	346	Large crack rear side hole (1). Crack forward side hole (1). Cracks both sides holes (2) and (3)
GZ2C7	6842	343	Same as GZ3C3

* Not used in any statistical comparisons of fatigue lives because of failure location.

TABLE 4(c)

Spectrum Type I: Specimens with 0·125 inch Diameter 2117 SLAN Rivets

Specimen number	Flights to failure	Failing load (kN)	Failure details
GK1B7	9362	300	Large crack rear side hole (1), crack forward side hole (1), small cracks at hole (2). See Fig. 5(*a*)
GK1D9	8642	348	Same as GK1B7 plus small crack at hole (3)
GK1E10	8542	403	Same as GK1B7
GN1D	9042	392	Same as GK1B7 plus small cracks at hole (3). See Fig. 5(*b*)
GN2R	15 442*	380	Failed through hole (8)
GN3B	8542	397	Large crack rear side hole (1), crack forward side hole (1), small cracks at holes (2) and (3)
GN4B	7742	374	Same as GN3B, except no cracks at hole (3)
GT10	9240	340	Same as GN3B
GT3F	7642	384	Same as GN3B
GT2G	7648	346	Same as GN4B. See Fig. 5(*c*)
GZ3A10	11 861	344	Same as GN3B
GZ3C8	8323	344	Same as GN4B. See Fig. 5(*d*)
GZ2A5	5058	268	Same as GN4B
GZ2C12	6940	319	Same as GN4B

* Not used in any statistical comparisons of fatigue lives because of failure location.

TABLE 4(a)

Spectrum Type I: Specimens with 2·5 mm Diameter A-U4G SLAN Rivets

Specimen number	Flights to failure	Failing load (kN)	Failure details
GK1A4	6642	Not recorded	Large crack rear side hole (1), crack forward side hole (1), small cracks at hole (2)
GK1B2	6342	374	Same as GK1A4
GK1C6	7342	351	Same as GK1A4
GK1D6	8742	370	Same as GK1A4 plus small cracks at hole (3)
GN10	8242	388	Same as GK1A4 plus small cracks at hole (3)
GN2E	6842	394	Same as GK1A4 plus small cracks at hole (3)

TABLE 4(b)

Spectrum Type I: Specimens with 3·0 mm Diameter A-U4G SLAN Rivets

Specimen number	Flights to failure	Failing load (kN)	Failure details
GN1P	7742	397	Large crack rear side hole (1), crack forward side hole (1), cracks at countersink of hole (2), small cracks at hole (3)
GN2G	9442	403	Same as GN1P
GN4C	4442	391	Same as GN1P
GN3A	4342	374	Same as GN1P
GN3E	8742	402	Same as GN1P
GN4E	6535	324	Same as GN1P
GT1G	6244	300	Same as GN1P
GZ3C10	6842	403	Same as GN1P
GZ3A11	8460	300	Same as GN1P
GZ2B10	9042	241	Same as GN1P
GZ2D8	5942	394	Same as GN1P

TABLE 3

Constant-Amplitude Fatigue Tests—Specimens with 0·125 inch 2117 SLAN Rivets

Specimen No.	Loading conditions	Cycles to failure	Failure details
GT1M	+7·5 g to −2·5 g	5420	At SLAN section
GN4P	at 1 Hz	3072	At SLAN section
GZ3D8		4245	At SLAN section
log. average life = 4135 cycles, s.d. log. life = 0·124			
GT1A	+6·5 g to −1·5 g	6450	At SLAN section
GN4M	at 1 Hz	8981	At SLAN section
GZ3B6		9410	At bolt hole (9)
GZ2D5		6666	At SLAN section
*log. average life = 8000 cycles, s.d. log. life = 0·087			
GT1E	+5·0 g to 0 g	56,870	At SLAN section
GN4L	at 3 Hz	53,470	At SLAN section
GZ3C4		57,360	At SLAN section
log. average life = 55,875 cycles, s.d. log. life = 0·017			
GT1J	+4·0 g to +0·5 g	222,350	At bolt hole (8)
GN40	at 3 Hz	130,160	At SLAN section
GZ3B4		163,560	At SLAN section
GZ2B12		138,080	At bolt hole (8)
*log. average life = 181,105 cycles, s.d. log. life = 0·111			
GT1R	+3·0 g to +1·0 g	839,530	At bolt hole (8)
GN4J	at 3 Hz	1,260,980	At bolt hole (9)
GZ3B12		1,340,080	Origin surface fretting near SLAN section
log. average life = 1,123,635 cycles, s.d. log. life = 0·110			

* Using Hald analysis, assuming failures at holes (8) and (9) represented "run-outs" at SLAN section.

TABLE 2

Spectrum Types

Cycles per 100 flights in Spectra Types I, II, III and IV					
Load levels and range (g)	I	Load levels and range (g)	II	III	IV
+7·5 to −2·5 (10)	1	+7·5 to −2·4 (9·9)	1	—	—
+6·5 to −1·5 (8)	38	+6·5 to −0·35 (6·85)	38	39	—
+5 to 0 (5)	400	+5 to +0·55 (4·45)	400	400	439
+4 to +0·5 (3·5)	450	+4 to +0·75 (3·25)	450	450	450
+3 to +1 (2)	1100	+3 to +1 (2)	1100	1100	1100
Total cycles per 100 flights	1989	—	1989	1989	1989

TABLE 1

Properties of Test Material

(*a*) *Chemical composition*

*Specification A7-U4SG (2214) (%)	Plate batch serial no. GK	GN	GT	GZ
Cu 3·9–5·0	4·56	4·40	4·26	4·43
Mg 0·2–0·8	0·38	0·33	0·35	0·36
Mn 0·4–1·2	0·62	0·60	0·66	0·62
Fe 0·30 max.	0·24	0·24	0·14	0·19
Si 0·5–1·2	0·73	0·77	0·73	0·72
Ti 0·15 max.	0·01	0·02	0·02	0·02
Cr 0·10 max.	Not analyzed			
Zn 0·25 max.	Not analyzed			

(*b*) *Static tensile*

	*Specification A7-U4SG-T651 (2214–T651)	Plate batch serial no. GK	GN	GT	GZ
0·1% proof stress (MPa)	—	440·5	444·7	449·5	450·8
0·1% proof stress (psi)		63,900	64,500	65,200	65,400
0·2% proof stress (MPa)	390	446·3	451·0	455·2	457·9
0·2% *proof stress (psi)*	56,600	64,700	65,400	66,000	66,400
Ultimate stress (MPa)	450	488·3	493·2	497·1	508·8
Ultimate stress (psi)	65,300	70,800	71,500	72,100	73,800
Elongation (%) $(5{\cdot}65\sqrt{A})$	5	10·1	12·3	11·4	11·5
0·1% PS/Ult	—	0·90	0·90	0·90	0·89

(*c*) *Fracture toughness*

	Plate batch serial no. GK (10 tests)		GN (11 tests)		GT (5 tests)		GZ (8 tests)		Pooled values (34 tests)	
	Average	s.d.	Average	s.d.	Average	s.d.	Average	s.d.	Average	s.d.
$MPa.m^{\frac{1}{2}}$	30·3	0·5	33·2	1·2	32·4	1·8	32·0	0·5	31·9	1·5
$ksi.in^{\frac{1}{2}}$	27·6	0·4	30·2	1·1	29·5	1·6	29·1	0·5	29·1	1·4

* *Conditions de controle des produits lamines en alliages d'aluminium utilises dans les constructions aerospatiales.* Ministere de la Defense, Direction Technique des Construction Aeronautiques AIR 9048, Edition No. 1, 26 December 1978, p. 91.

APPENDIX

Fractographic Crack Growth Measurements

Each fracture was examined using three independent techniques:

(i) a macrophotograph at about $\times 15$ magnification to provide crack growth data at relatively large crack depths;

(ii) an optical stereo microscope with diffuse illumination and magnification of $\times 100$, 50 and 25; and

(iii) a metallographic microscope with polarized vertical illumination, using magnifications of $\times 500$ or 50.

Both microscopes were fitted with a cross-hair in one eye piece. The specimens were mounted on an X–Y stage fitted with photo-electric digital micrometers reading to 0·001 mm, and the crack depths corresponding to the applications of the 7·5 g load were accurately measured by traversing the specimens under the microscope objectives. Whenever possible the traverse of the fracture surface was perpendicular to the axis of the hole.

Because of the substantial overlapping of the region of the fracture by each independent visualization technique about 80% of the crack depth data were duplicated. However, measurements obtained using the metallographic microscope were considered to be the most accurate at short crack depths ($\times 500$) and large crack depths ($\times 50$), and those using the stereo microscope the most accurate at intermediate crack depths. Thus the crack depth versus life data presented are not a simple average of the measurements obtained by the different techniques but represent the actual measurements obtained using the technique considered to be most accurate over particular regions of the fracture. When combined together they provided a coherent set of data covering the entire line of traverse.

As a check on the validity of the interpretation of the individual fracture markings on each specimen all the data obtained for a particular fracture using the three independent techniques were combined and examined on the basis of a relationship between crack depth and incremental crack growth. For intermediate and large crack depths (i.e. for greater than about 0·5 mm) this relationship was found to be approximately linear. On the relatively rare occasions when individual measurements indicated wide departures from this relationship the particular data were reassessed. When data could not be validated by independent measurements using more than one technique (about 20% of the data), the validity of individual measurements in such cases were assessed by the individual relationship between crack depth and incremental crack growth.

TABLE 10 [Continued]

Specimen No.	GZ3A10	GK1E10	GN3B	GN4B	GK1B7	GN1D	GT2G	GZ2C12	GZ3C8	GT10	GT3F	GK1D9	GZ2A5
Crack depth (mm)	Flights (N_n) to given crack depth and then to failure ( )												
2·0	7805 (4056)	6502 (2040)	5999 (2543)	4816 (2926)	7430 (1932)	5471 (3571)	5184 (2464)	4364 (2576)	5563 (2760)	6930 (2310)	6062 (1580)	6237 (2405)	2563 (2495)
2·5	8564 (3297)	6838 (1704)	6564 (1978)	5290 (2452)	7988 (1374)	5961 (3081)	5644 (2004)	4818 (2122)	6060 (2263)	7240 (2000)	6388 (1254)	6572 (2070)	2857 (2201)
3·0	9271 (2590)	7135 (1407)	6944 (1598)	5702 (2040)	8335 (1027)	6433 (2609)	6001 (1647)	5164 (1776)	6488 (1835)	7557 (1683)	6606 (1036)	6852 (1790)	3135 (1923)
3·5	9773 (2088)	7405 (1137)	7277 (1265)	6086 (1656)	8616 (746)	6837 (2205)	6282 (1366)	5435 (1505)	6787 (1536)	7817 (1423)	6794 (848)	7102 (1540)	3364 (1694)
4·0	10131 (1730)	7654 (888)	7538 (1004)	6403 (1339)	8833 (529)	7266 (1776)	6547 (1101)	5669 (1271)	7007 (1316)	8043 (1197)	6985 (657)	7337 (1305)	3563 (1495)
4·5	10414 (1447)	7872 (670)	7750 (792)	6659 (1083)	9009 (353)	7590 (1452)	6737 (911)	5845 (1095)	7213 (1110)	8237 (1003)	7149 (493)	7549 (1093)	3733 (1325)
5·0	10661 (1200)	8043 (499)	7899 (643)	6862 (880)	9161 (201)	7863 (1179)	6914 (734)	6000 (940)	7403 (920)	8418 (822)	7270 (372)	7731 (911)	3890 (1168)
5·5	10870 (991)	8161 (381)	8015 (527)	7008 (734)	9280 (82)	8105 (937)	7071 (577)	6137 (803)	7541 (782)	8554 (686)	7369 (273)	7875 (767)	4034 (1024)
Failure	11861	8542	8542	7742	9362	9042	7648	6940	8323	9240	7642	8642	5058

TABLE 11

Variability in Fatigue Crack Formation and Growth

Crack depth (mm)	Specimens in sample	Logarithmic			Arithmetic			Lives to ±1 standard deviation			
		Mean	Standard deviation	Coefficient of variation	Mean	Standard deviation	Coefficient of variation	Logarithmic		Arithmetic	
								−1 s.d.	+1 s.d.	−1 s.d.	+1 s.d.
0·3	10	3038 (5511)	·127 (·066)	·036 (·018)	3155 (5570)	902 (882)	·286 (·158)	2267 (4739)	4069 (6409)	2253 (4688)	4057 (6452)
0·4	10	3324 (5223)	·122 (·068)	·035 (·018)	3441 (5283)	940 (871)	·273 (·165)	2510 (4466)	4401 (6109)	2501 (4412)	4381 (6154)
0·5	10	3563 (4982)	·119 (·070)	·034 (·019)	3682 (5042)	979 (853)	·266 (·169)	2710 (4241)	4684 (5851)	2703 (4189)	4661 (5895)
1·0	10	4563 (4011)	·103 (·080)	·028 (·022)	4650 (4074)	1076 (789)	·231 (·194)	3579 (3373)	5750 (4820)	3574 (3285)	5727 (4863)
1·5	10	5294 (3261)	·093 (·087)	·025 (·025)	5402 (3322)	1132 (703)	·210 (·212)	4278 (2668)	6551 (3985)	4270 (2620)	6534 (4025)
2·0	10	5910 (2652)	·083 (·100)	·022 (·029)	6006 (2718)	1137 (660)	·189 (·243)	4887 (2107)	7147 (3338)	4869 (2058)	7143 (3378)

TABLE 11 [Continued]

Crack depth (mm)	Specimens in sample	Logarithmic			Arithmetic			Lives to ±1 standard deviation			
		Mean	Standard deviation	Coefficient of Variation	Mean	Standard deviation	Coefficient of Variation	Logarithmic		Arithmetic	
								−1 s.d.	+1 s.d.	−1 s.d.	+1 s.d.
2·5	10	6401 (2161)	·079 (·113)	·026 (·034)	6497 (2228)	1186 (587)	·183 (·263)	5341 (1668)	7672 (2800)	5311 (1640)	7682 (2815)
3·0	10	6806 (1761)	·077 (·120)	·020 (·040)	6903 (1821)	1239 (490)	·179 (·269)	5707 (1337)	8117 (2321)	5664 (1331)	8142 (2311)
3·5	10	7135 (1434)	·075 (·134)	·019 (·042)	7232 (1493)	1271 (428)	·176 (·287)	6011 (1054)	8470 (1951)	5960 (1065)	8503 (1921)
4·0	10	7415 (1156)	·072 (·152)	·019 (·050)	7509 (1215)	1282 (372)	·171 (·306)	6279 (815)	8756 (1640)	6228 (843)	8791 (1587)
4·5	10	7639 (928)	·071 (·180)	·018 (·061)	7733 (992)	1295 (335)	·167 (·338)	6489 (613)	8993 (1406)	6438 (657)	9027 (1327)
5·0	10	7829 (728)	·070 (·227)	·018 (·079)	7922 (802)	1308 (302)	·165 (·377)	6666 (431)	9196 (1229)	6614 (499)	9231 (1104)
5·5	10	7981 (555)	·069 (·317)	·018 (·116)	8074 (650)	1320 (271)	·163 (·417)	6808 (268)	9357 (1152)	6754 (379)	9395 (921)
Failure	10	8639	·063	·016	8724	1339	·153	7471	9990	7385	10063

Figures in parentheses refer to propagation lives.

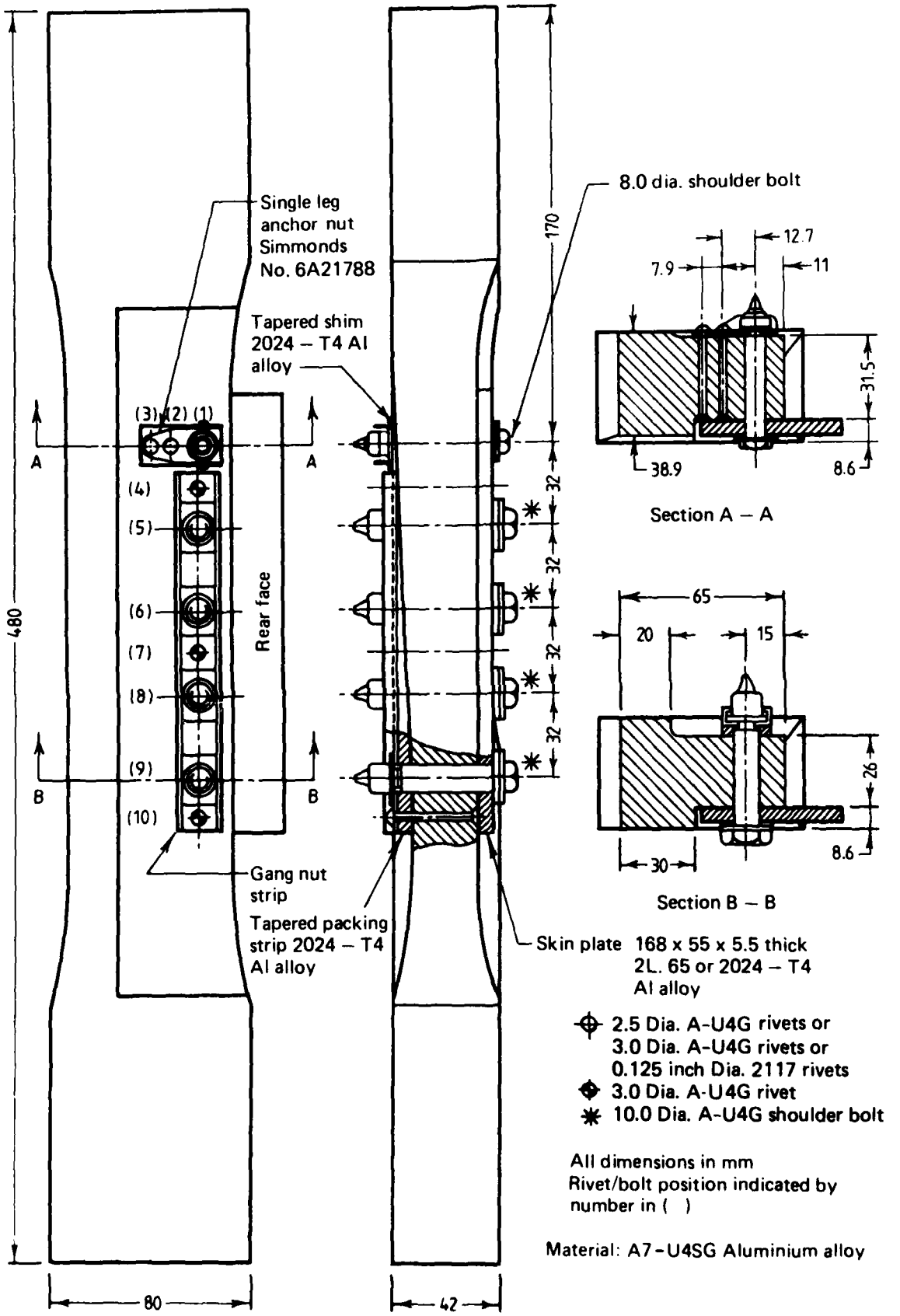

FIG. 1 MIRAGE SPAR LOWER REAR FLANGE FATIGUE SPECIMEN

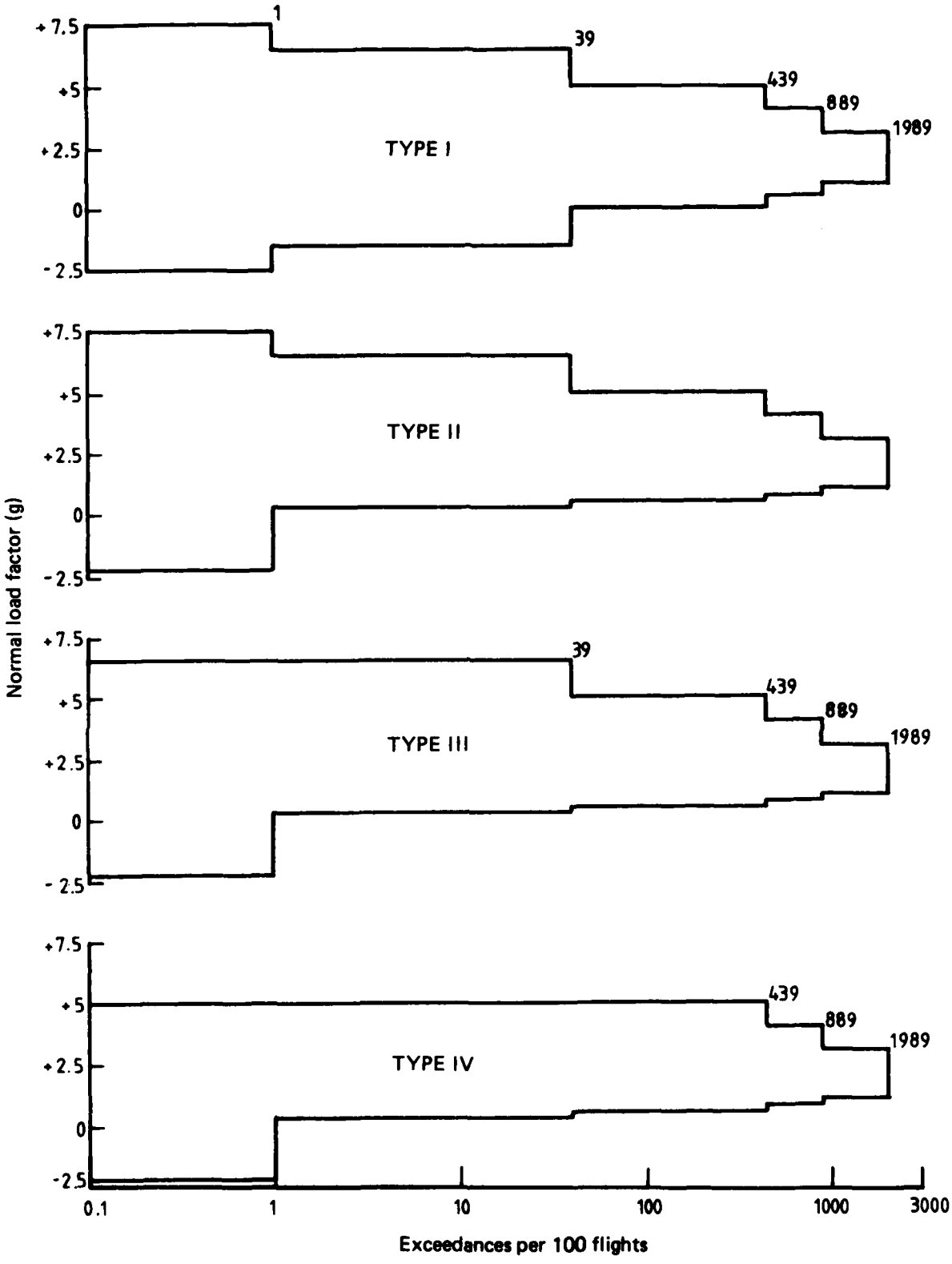

FIG. 2 FATIGUE TEST SPECTRA

100 FLIGHTS (1989 CYCLES) REPRESENT 66.6 HOURS OF FLYING

FLIGHT A' →	10 CYCLES +3g/+1g	5 CYCLES +4g/+0.5g	2 CYCLES +5g/0g	1 CYCLE +6.5g/-1.5g	1 CYCLE +7.5g/-2.5g	1 CYCLE +6.5g/-1.5g	2 CYCLES +5g/0g	4 CYCLES +4g/+0.5g	10 CYCLES +3g/+1g

FLIGHT A →	10 CYCLES +3g/+1g	2 CYCLES +4g/+0.5g	2 CYCLES +5g/0g	2 CYCLES +6.5g/-1.5g	2 CYCLES +5g/0g	2 CYCLES +4g/+0.5g	5 CYCLES +3g/+1g

FLIGHT B →	5 CYCLES +3g/+1g	5 CYCLES +4g/+0.5g	9 CYCLES +5g/0g	4 CYCLES +4g/+0.5g	5 CYCLES +3g/+1g

FLIGHT C →	5 CYCLES +3g/+1g	1 CYCLE +4g/+0.5g	5 CYCLES +3g/+1g

CYCLES OF +6.5g/-1.5g AND
+7.5g/-2.5g AT 1 Hz;
REMAINDER OF CYCLES AT 3 Hz

SEQUENCE OF FLIGHTS IN 100 FLIGHTS: 1 FLIGHT A', 18 FLIGHTS A, 36 FLIGHTS B AND 45 FLIGHTS C

1	2	3	4	5	6	7	8	9	10	11	12	13	14	15	16	17	18	19	20	21	22	23	24	25	26	27	28	29	30	31	32	33	34	35	36	37	38	39	40	41	42	43	44	45	46	47	48	49	50
B	C	C	B	C	C	C	A	C	C	B	B	A	C	C	C	B	A	C	B	B	B	A	C	C	C	A	A	C	C	B	B	B	C	B	A	B	C	C	B	A	A'	B	C	C	A	A	B	B	C
51	52	53	54	55	56	57	58	59	60	61	62	63	64	65	66	67	68	69	70	71	72	73	74	75	76	77	78	79	80	81	82	83	84	85	86	87	88	89	90	91	92	93	94	95	96	97	98	99	100
C	B	C	C	B	C	B	B	C	C	C	A	B	A	C	C	C	B	A	B	B	B	C	B	C	C	A	B	C	B	A	B	C	C	B	A	A	B	C	C	B	C	C	B	B	C	B	C	A	C

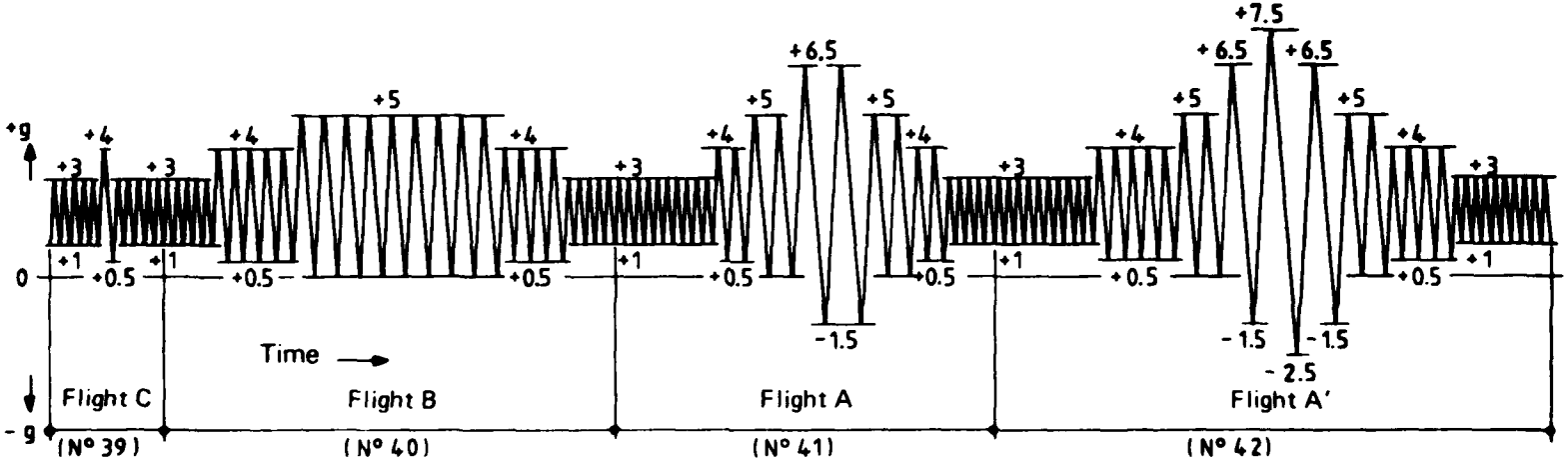

FIG. 3 FRENCH 100 FLIGHT MIRAGE III FLIGHT-BY-FLIGHT SEQUENCE

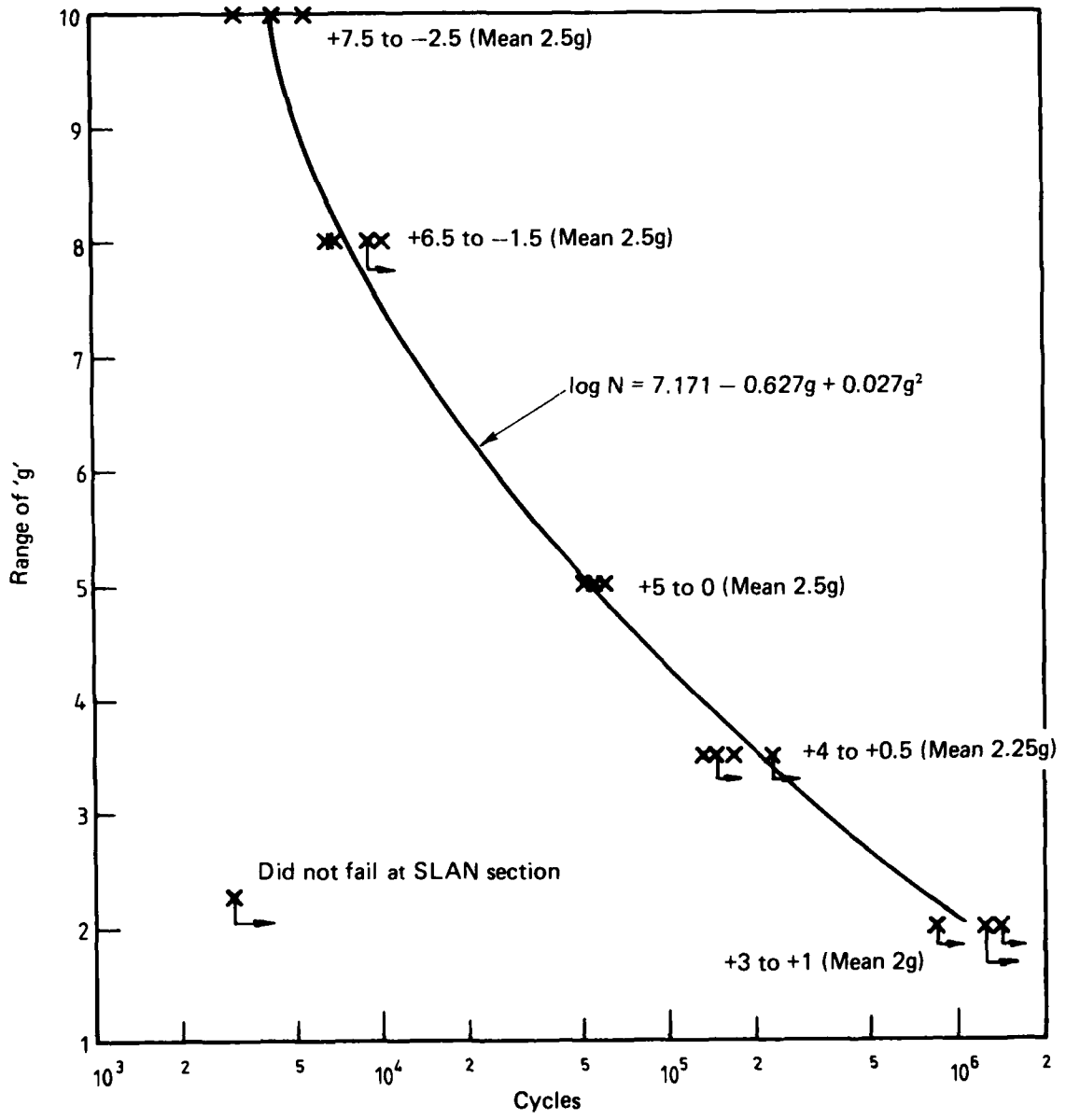

FIG. 4 S/N DIAGRAM FOR CONSTANT – AMPLITUDE TESTS

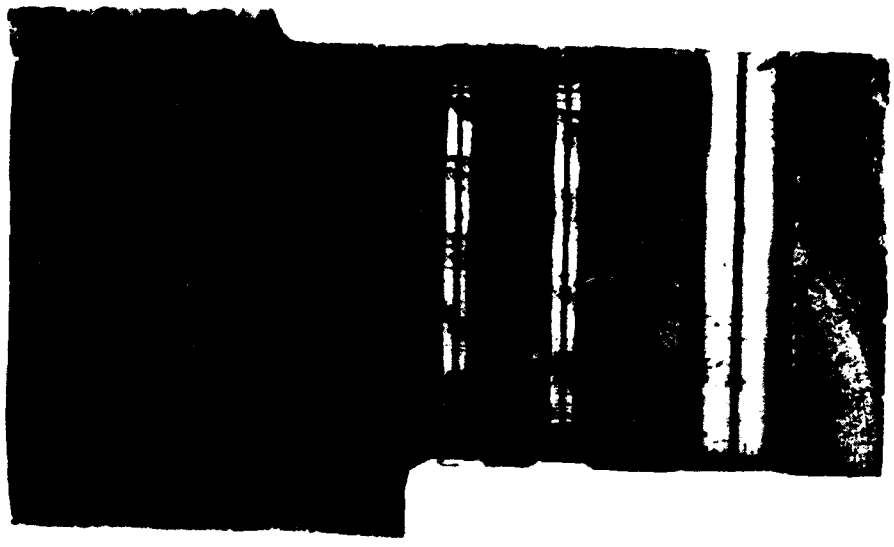

(a) Specimen GK1B7, 9362 flights spectrum TYPE I

(b) Specimen GN1D, 9042 flights spectrum TYPE I

FIG. 5 FATIGUE FRACTURE SURFACES

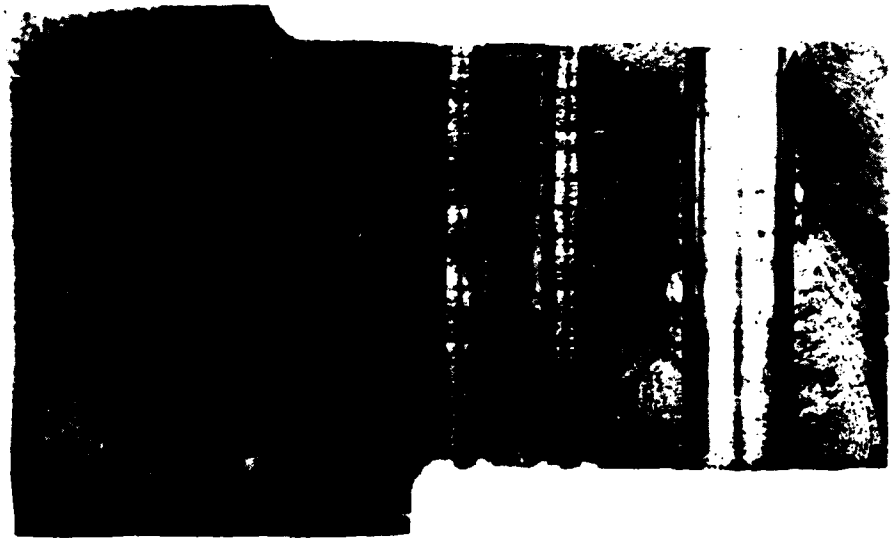

(c) Specimen GT2G, 7648 flights spectrum TYPE I

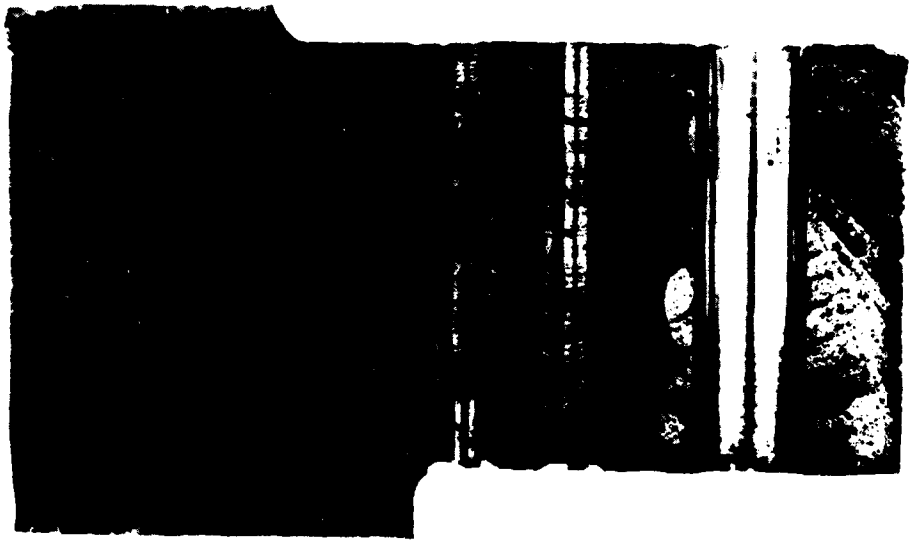

(d) Specimen GZ3C8, 8323 flights spectrum TYPE I

FIG. 5 (cont.) FATIGUE FRACTURE SURFACES

FIG. 6 ELECTRON FRACTOGRAPH SPECIMEN GN1O
Arrows indicate occurrence of +7.5g load.

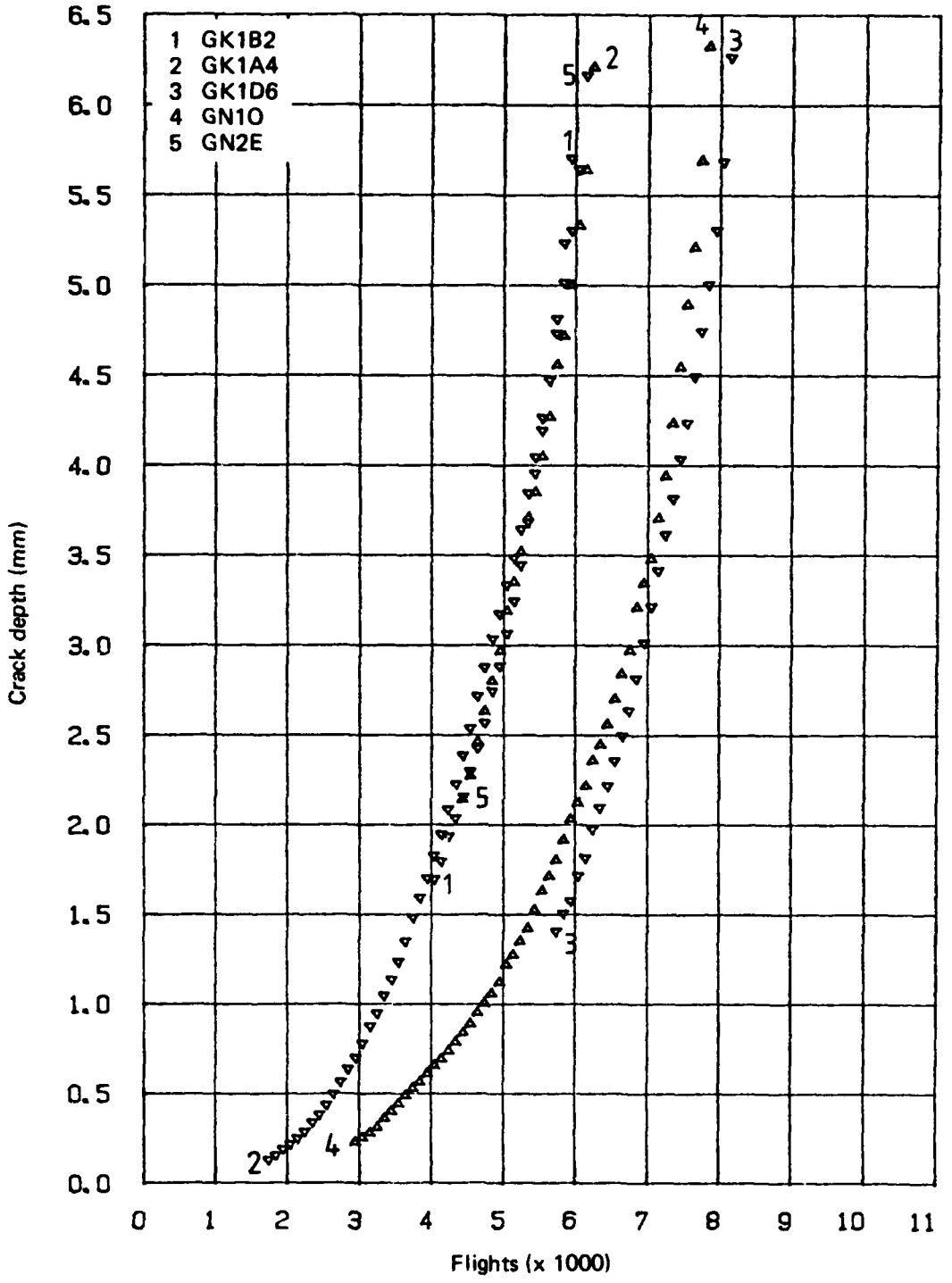

FIG. 7(a) FATIGUE CRACK GROWTH FROM 8 mm BOLT HOLE – SPECIMENS WITH 2.5 mm SLAN RIVETS

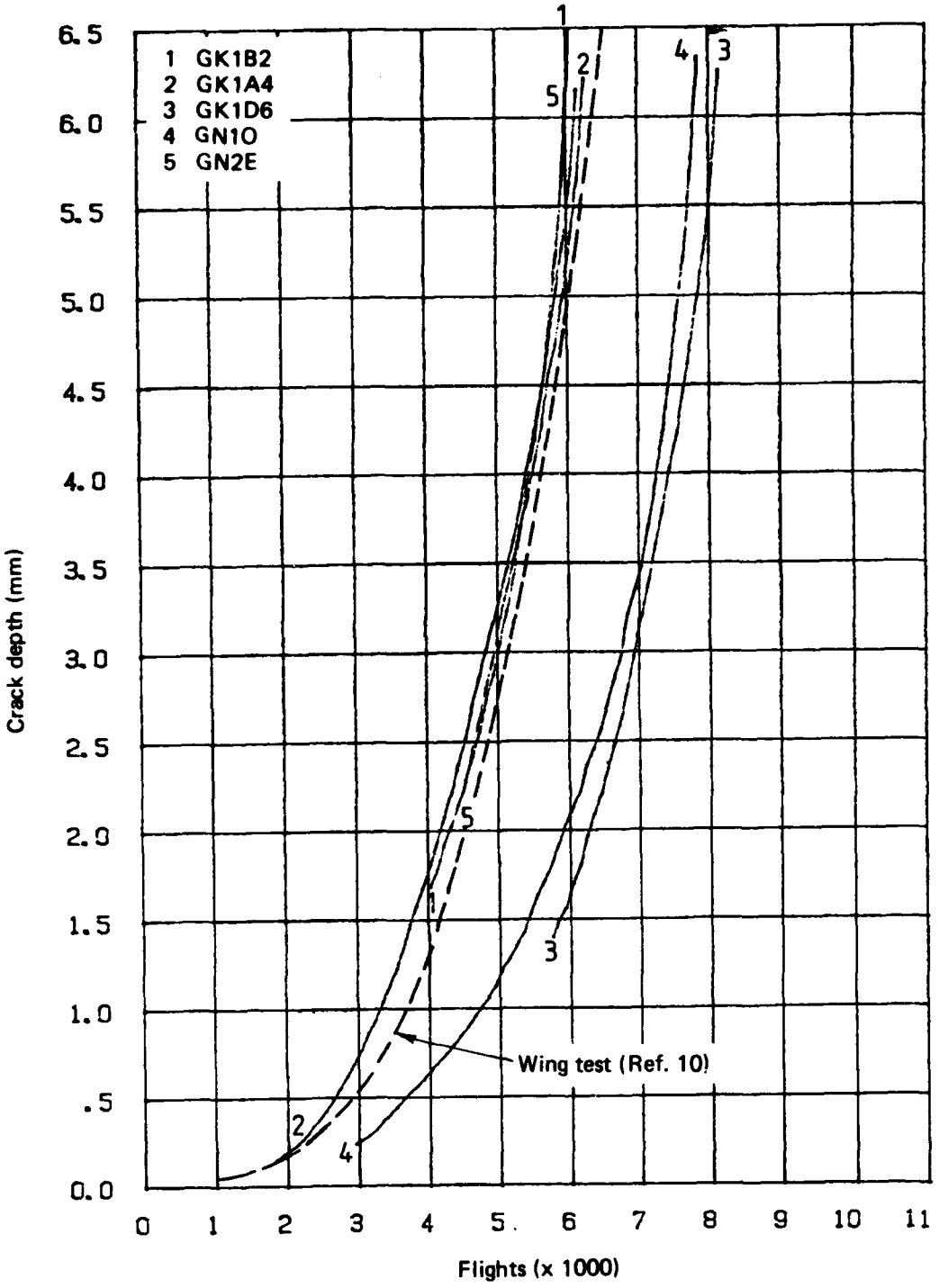

FIG. 7(b) FATIGUE CRACK GROWTH FROM 8 mm BOLT HOLE – SPECIMENS WITH 2.5 mm SLAN RIVETS

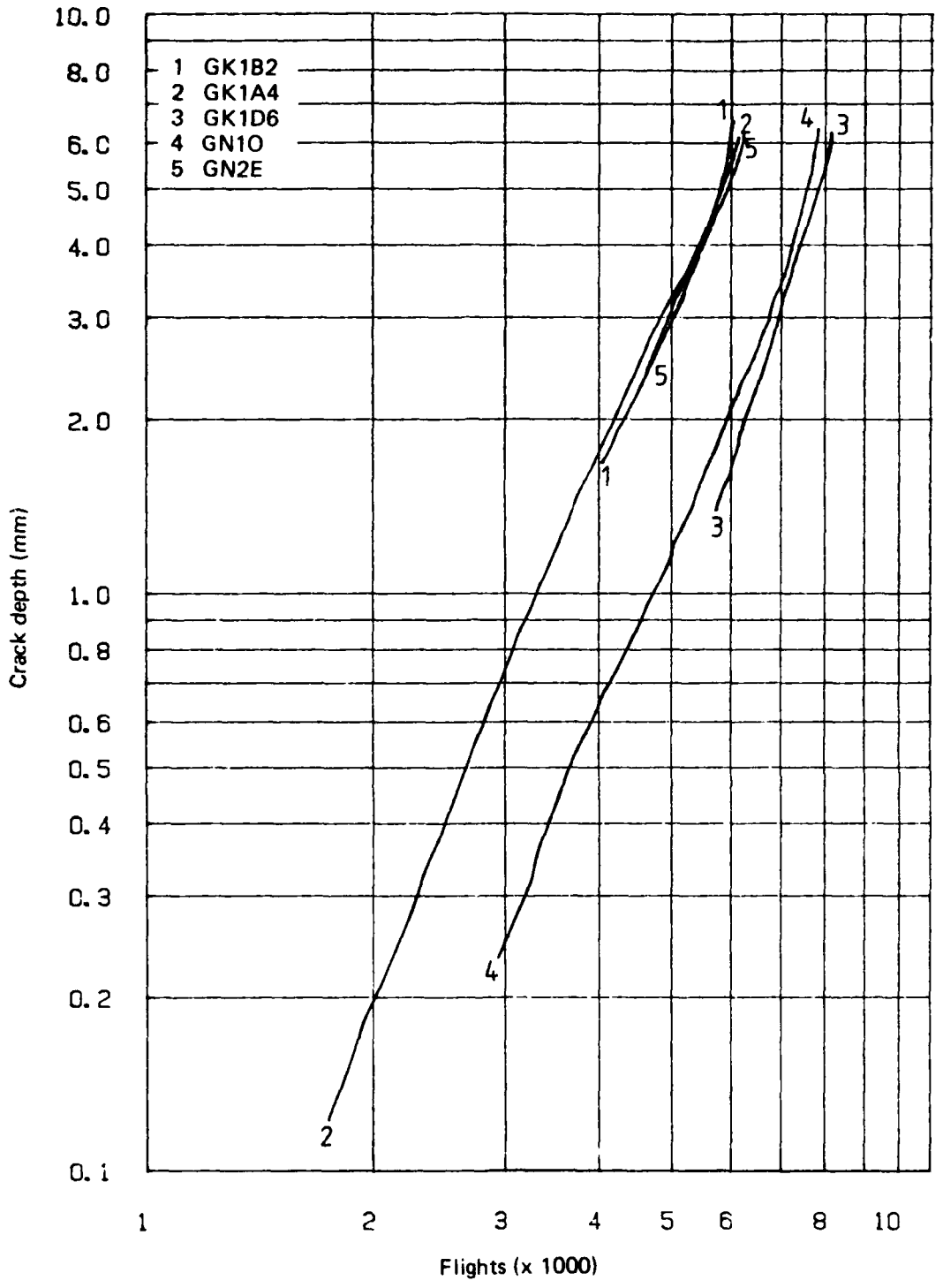

FIG. 7(c) FATIGUE CRACK GROWTH FROM 8 mm BOLT HOLE — SPECIMENS WITH 2.5 mm SLAN RIVETS

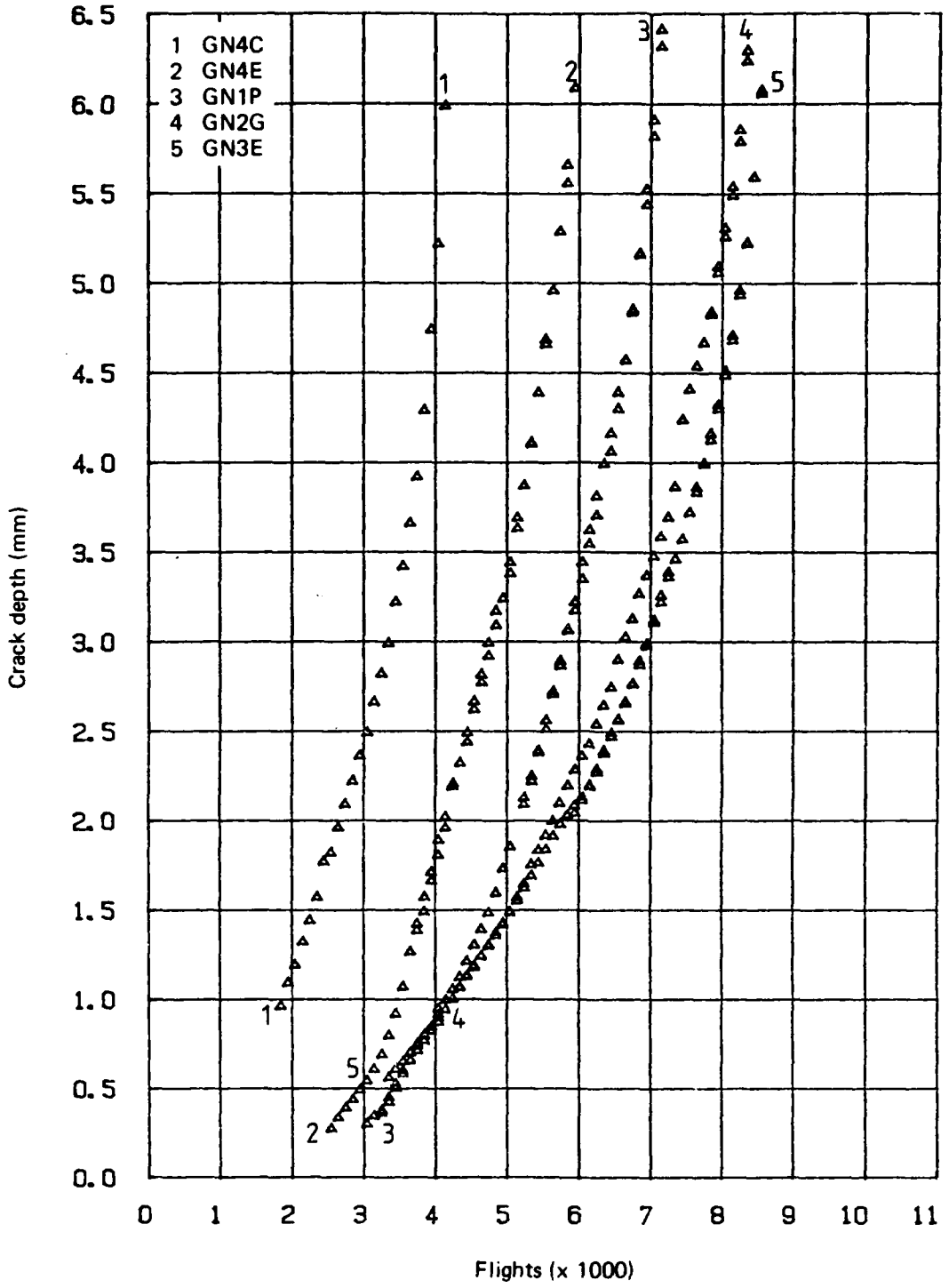

FIG. 8(a) FATIGUE CRACK GROWTH FROM 8 mm BOLT HOLE – SPECIMENS WITH 3.0 mm SLAN RIVETS

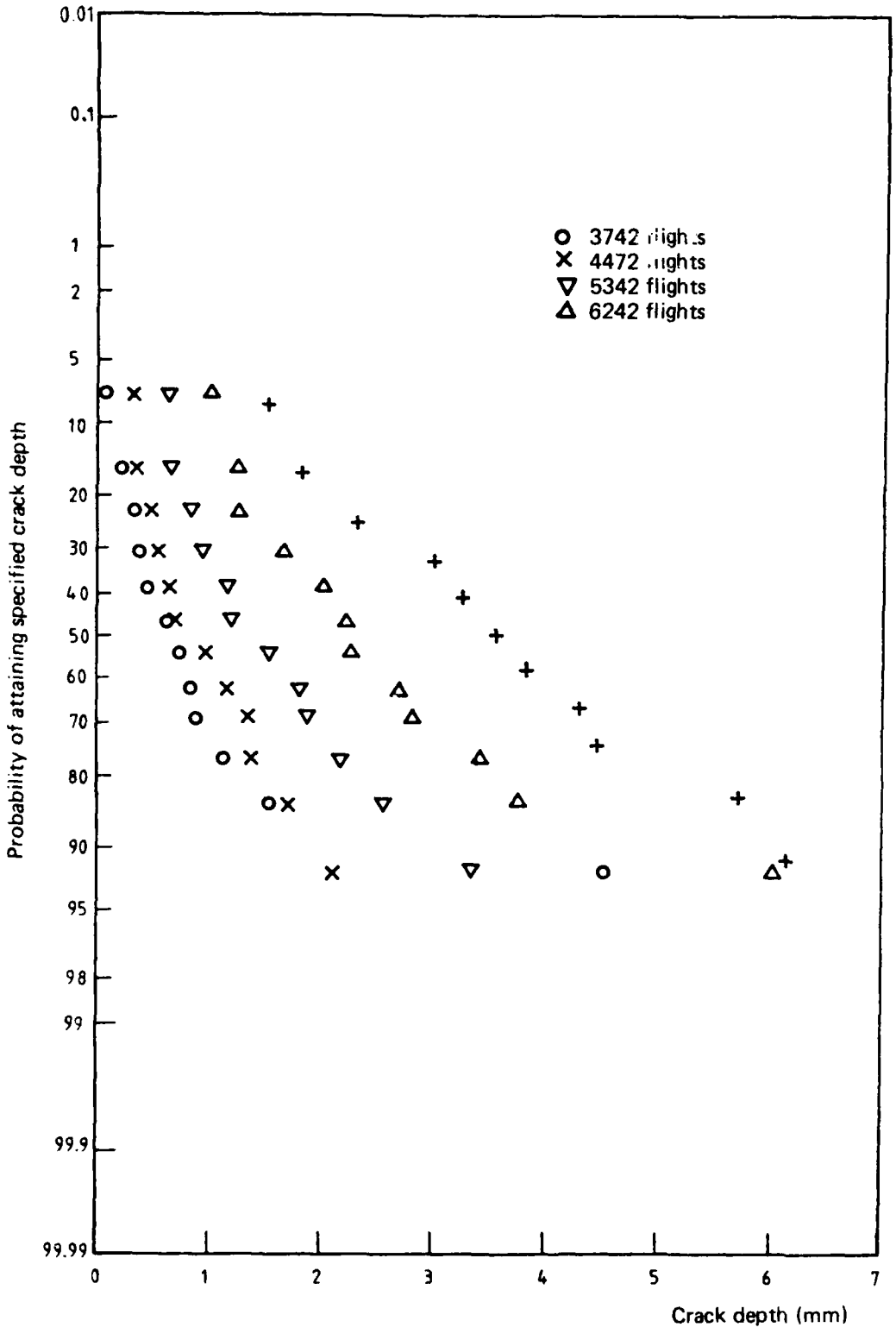

FIG. 12(a) PROBABILITY DISTRIBUTION OF CRACK DEPTHS AT DIFFERENT LIVES

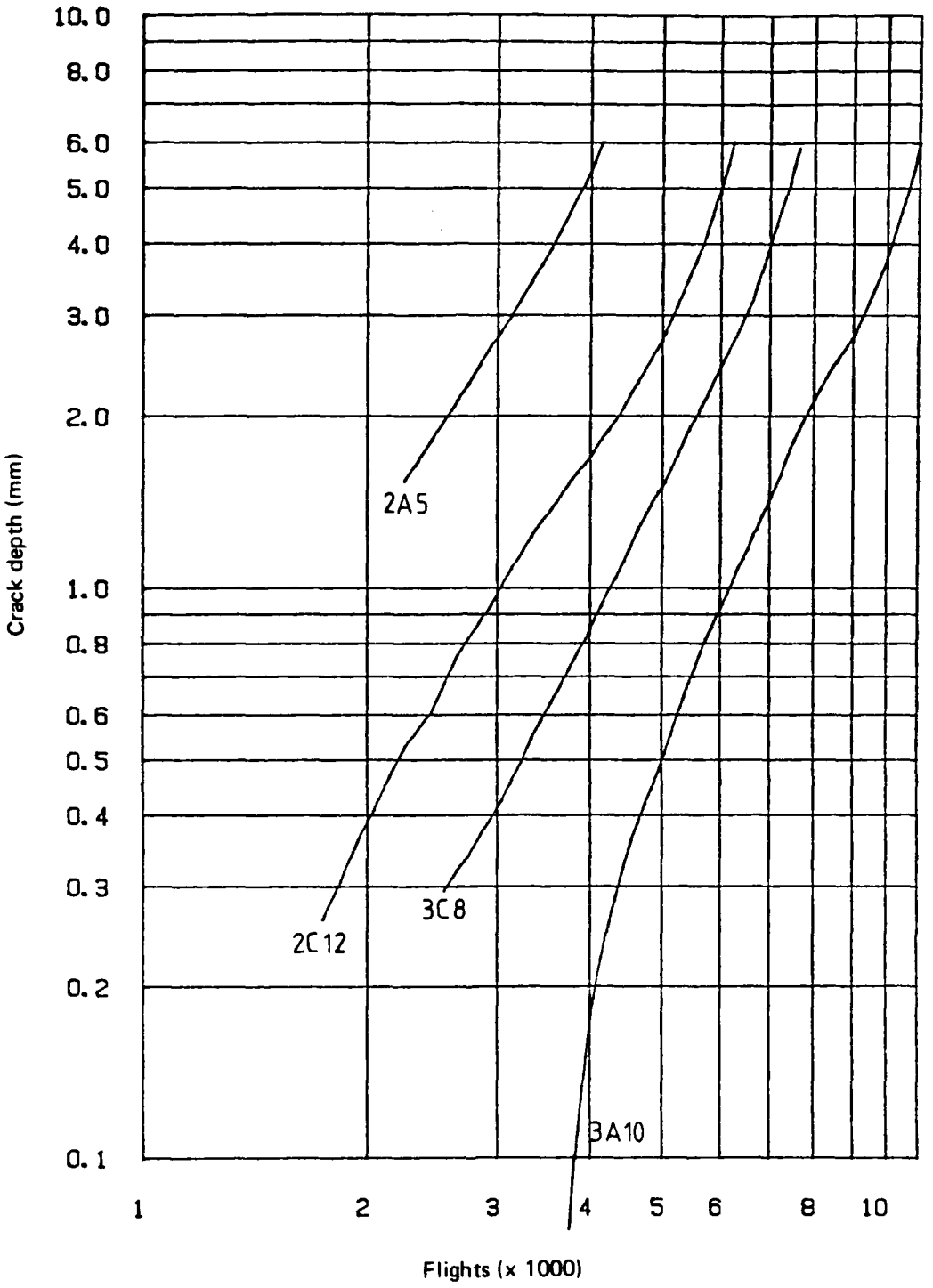

FIG. 11(d) FATIGUE CRACK GROWTH – SPECIMENS WITH 0.125 INCH SLAN RIVETS, SPECTRUM TYPE I, MATERIAL BATCH GZ

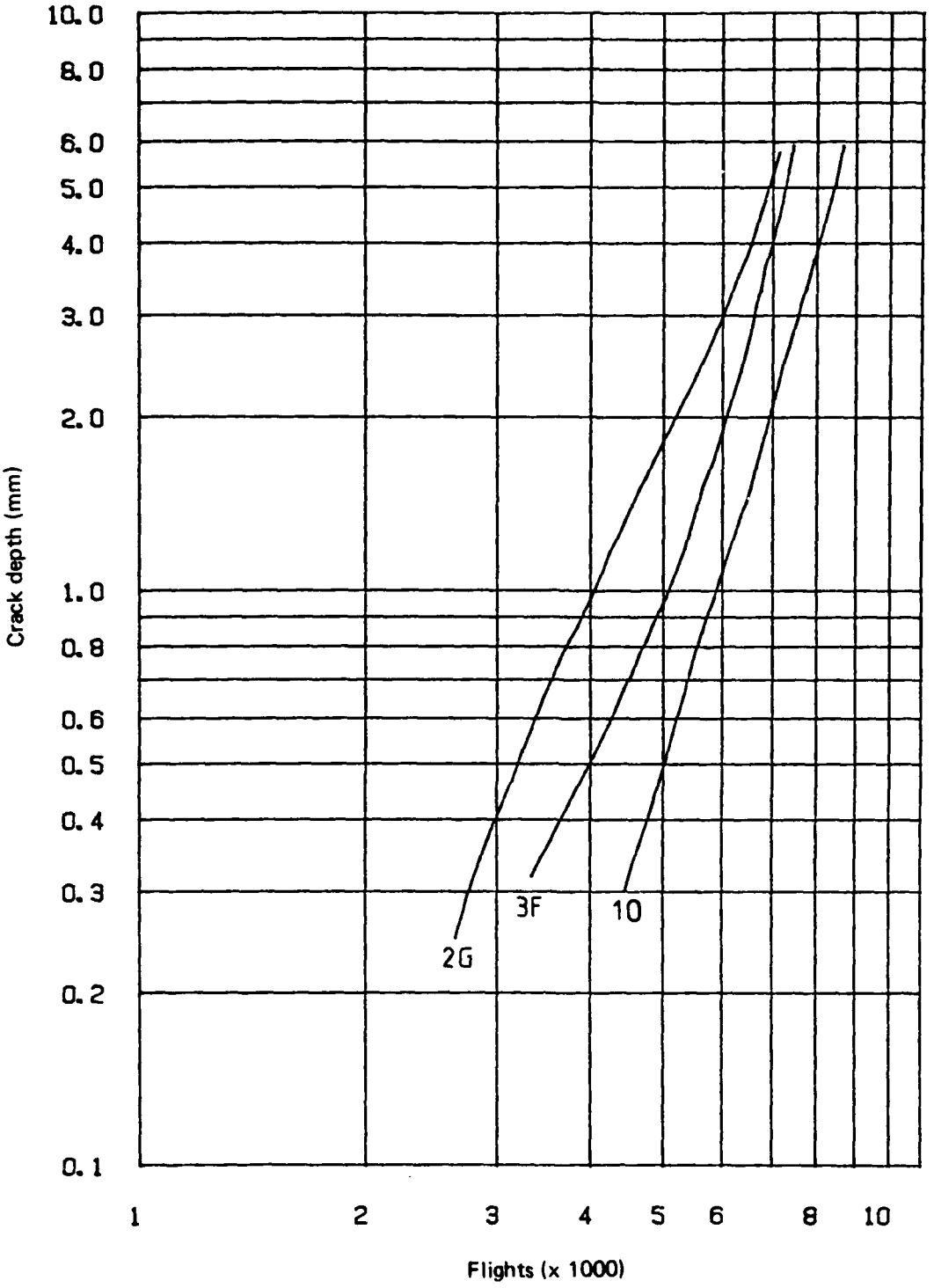

FIG. 11(c) FATIGUE CRACK GROWTH – SPECIMENS WITH 0.125 INCH SLAN RIVETS, SPECTRUM TYPE I, MATERIAL BATCH GT

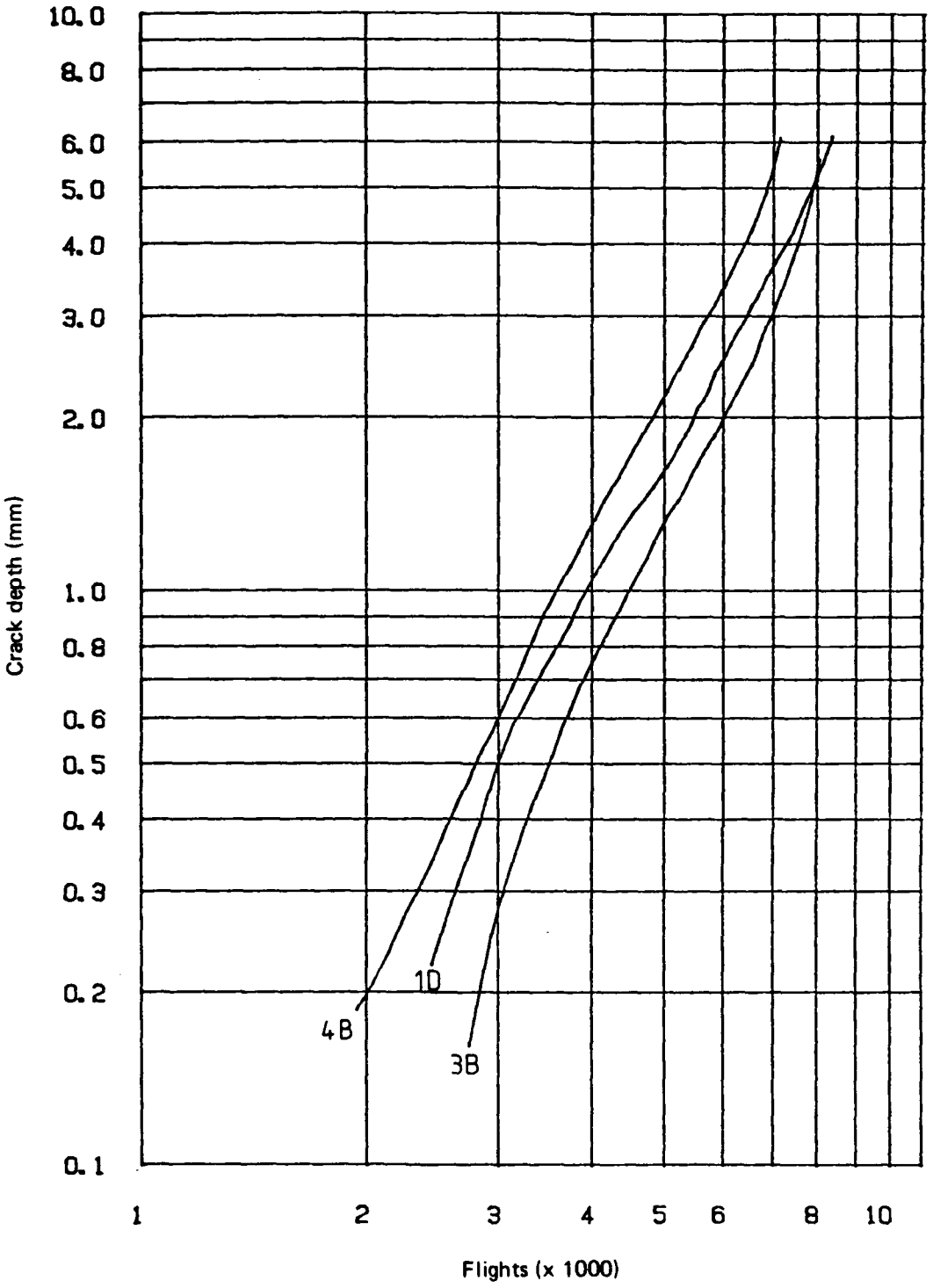

FIG. 11(b) FATIGUE CRACK GROWTH – SPECIMENS WITH 0.125 INCH SLAN RIVETS, SPECTRUM TYPE I, MATERIAL BATCH GN

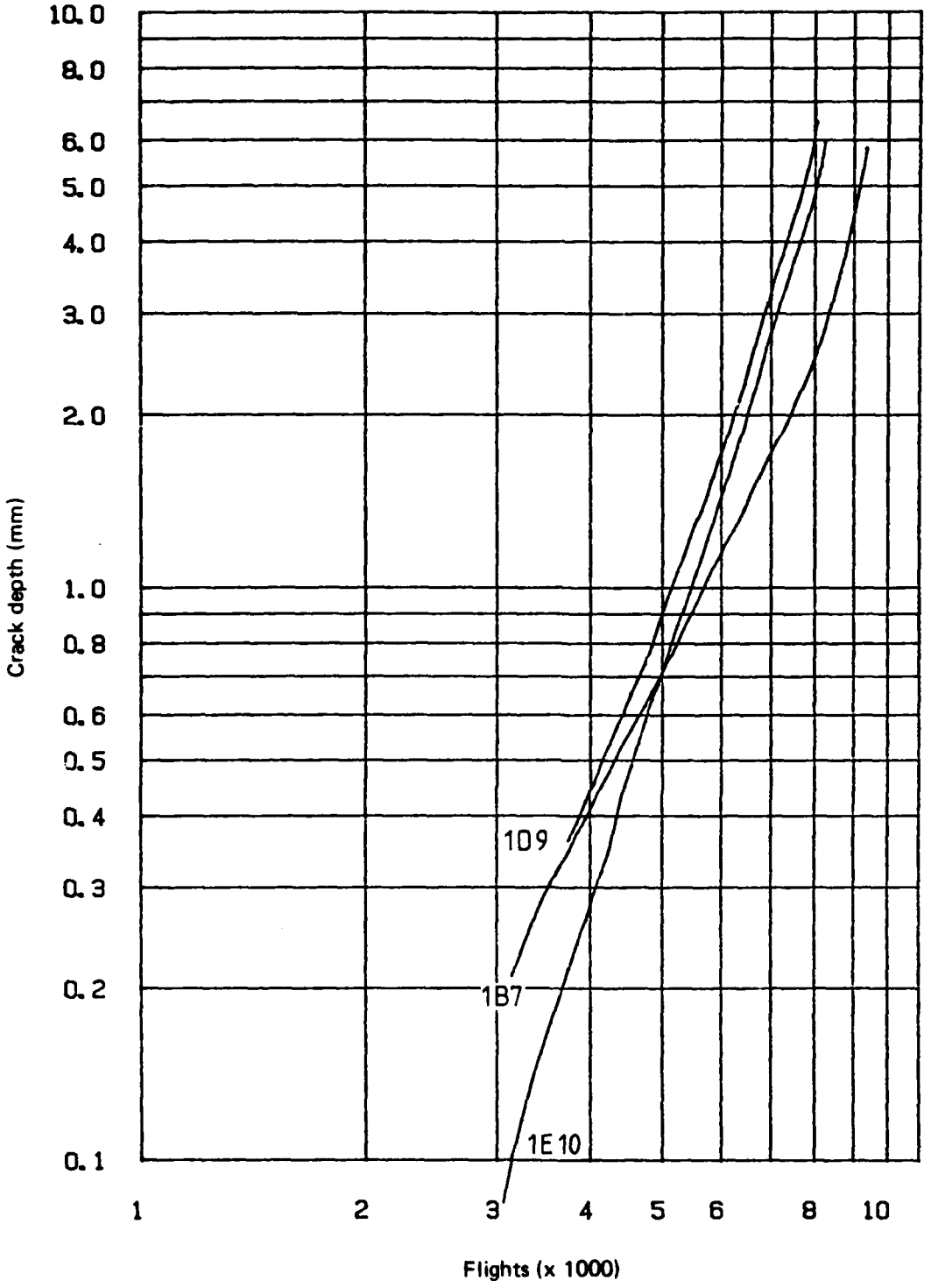

FIG. 11(a) FATIGUE CRACK GROWTH – SPECIMENS WITH 0.125 INCH SLAN RIVETS, SPECTRUM TYPE I, MATERIAL BATCH GK

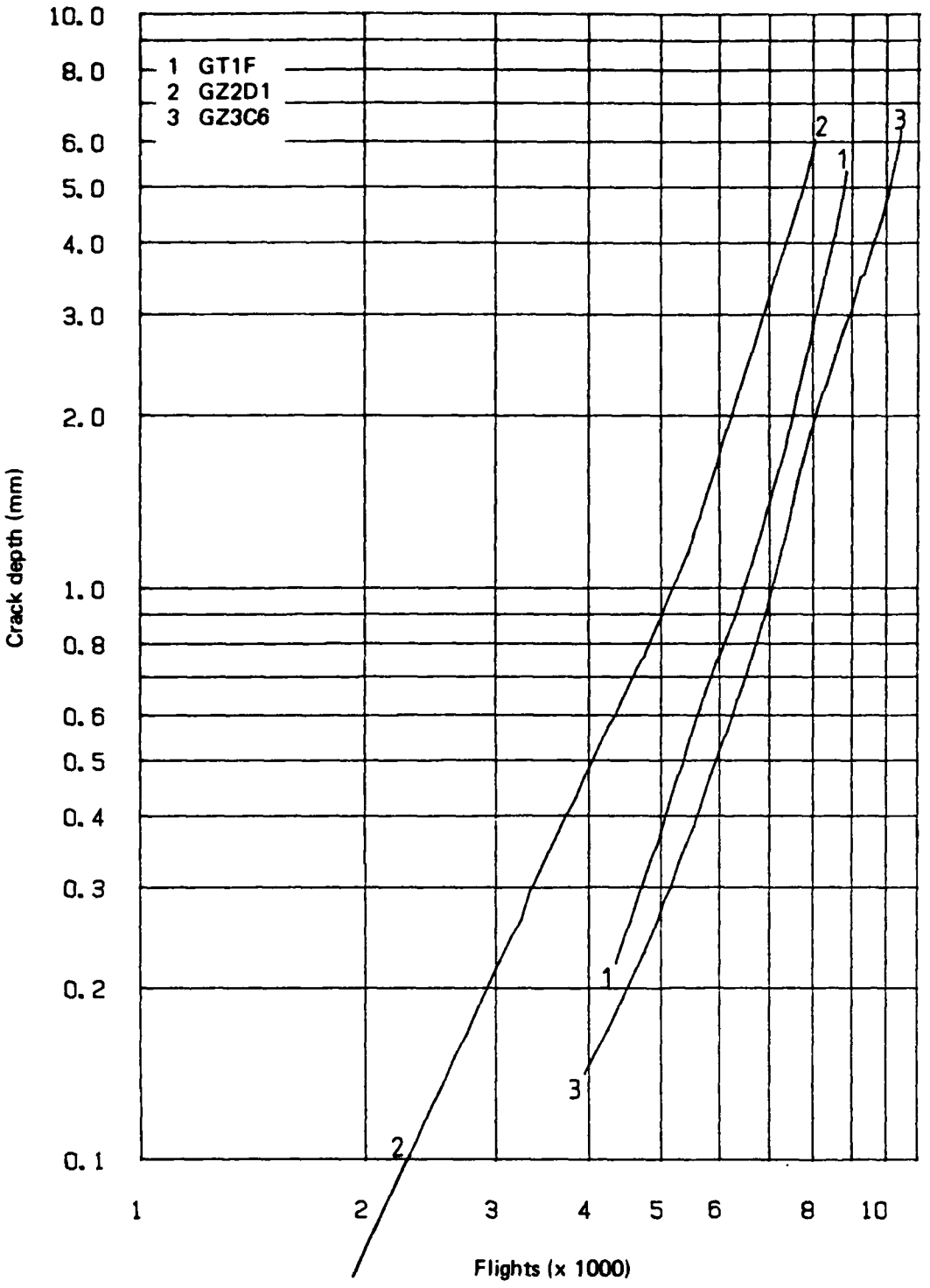

FIG. 10(c) FATIGUE CRACK GROWTH FROM 8 mm BOLT HOLE – SPECIMENS WITH 0.125 INCH SLAN RIVETS, SPECTRUM TYPE II

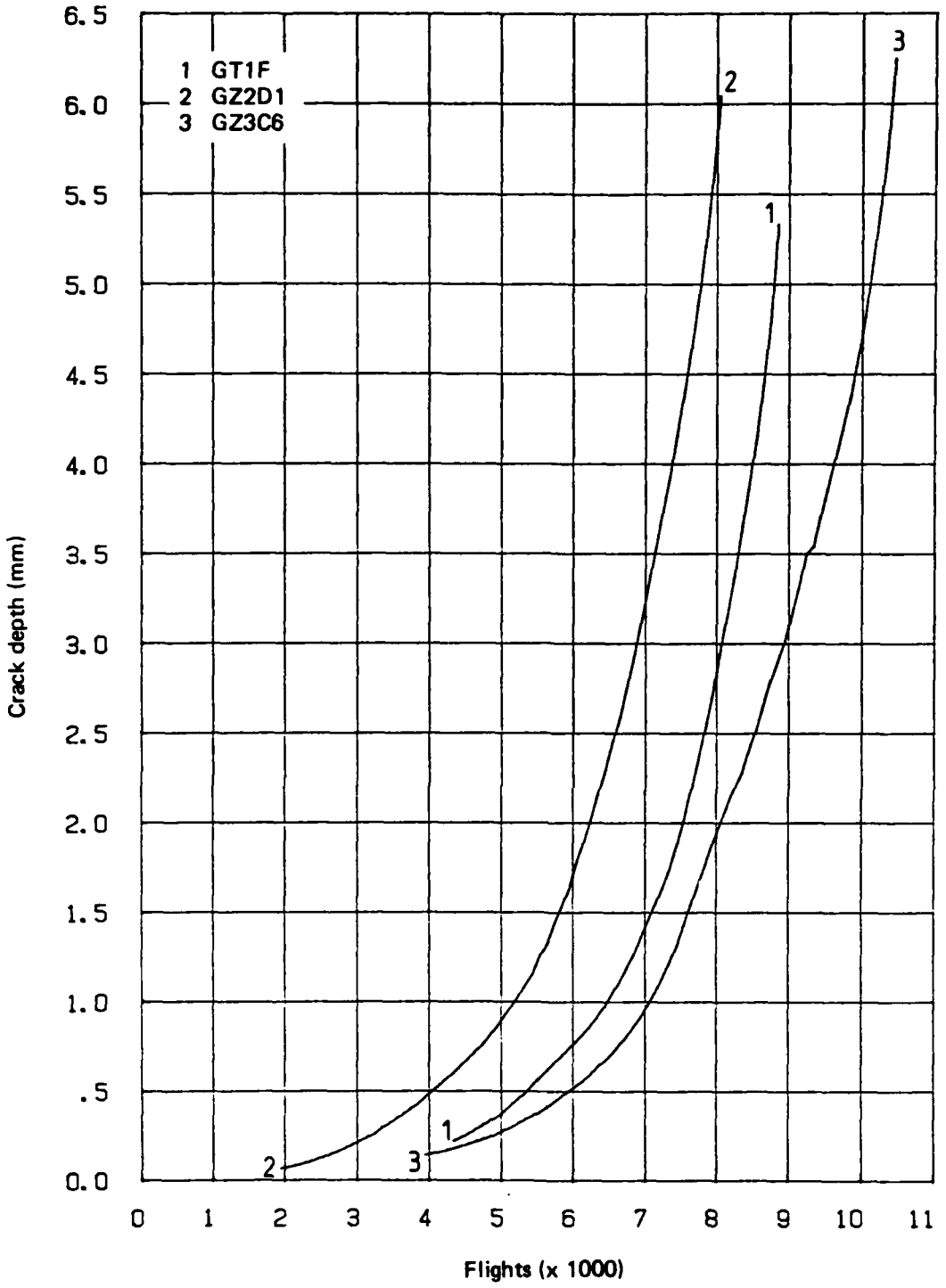

FIG. 10(b) FATIGUE CRACK GROWTH FROM 8 mm BOLT HOLE – SPECIMENS WITH 0.125 INCH SLAN RIVETS, SPECTRUM TYPE II

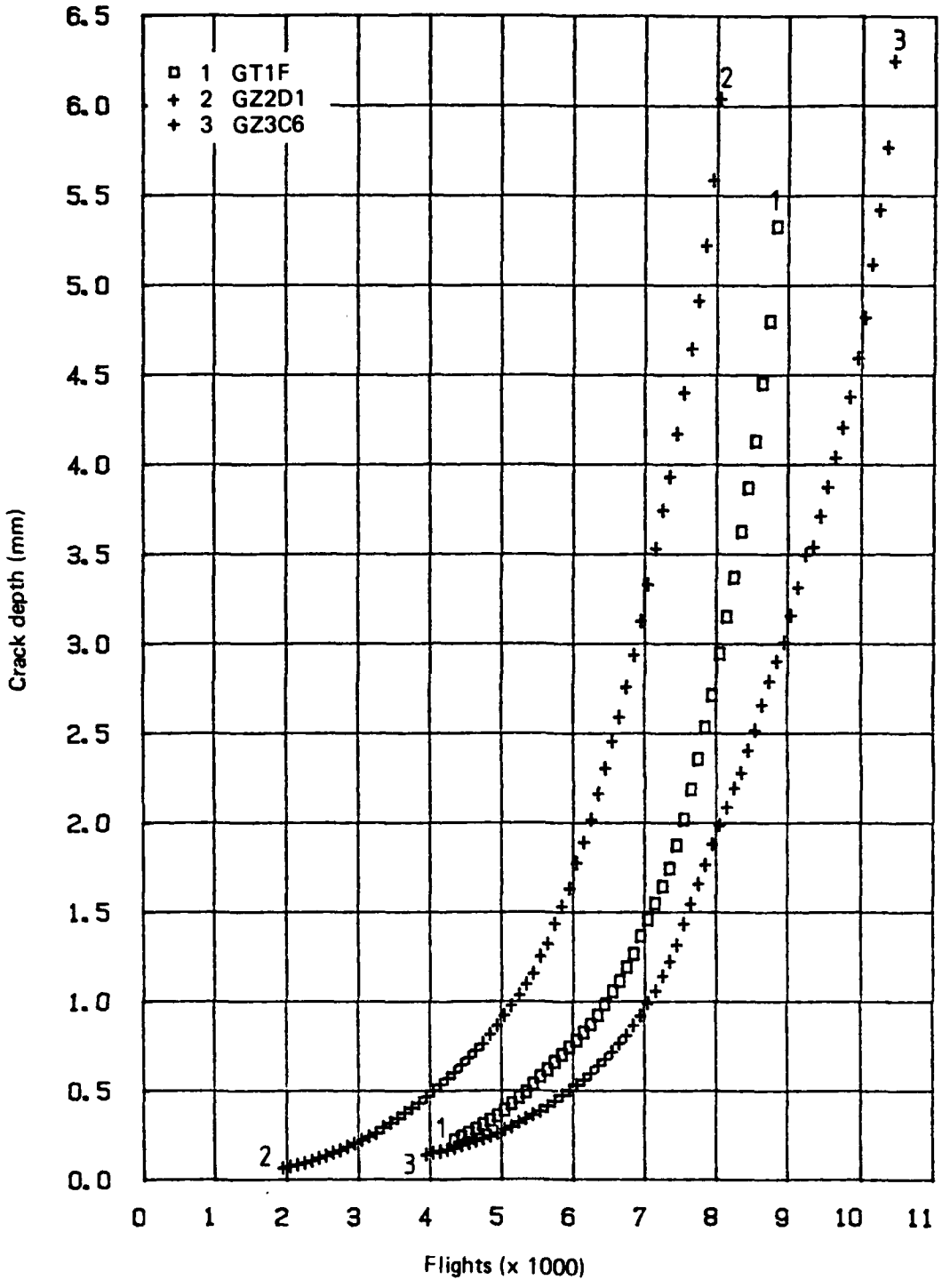

FIG. 10(a) FATIGUE CRACK GROWTH FROM 8 mm BOLT HOLE – SPECIMENS WITH 0.125 INCH SLAN RIVETS, SPECTRUM TYPE II

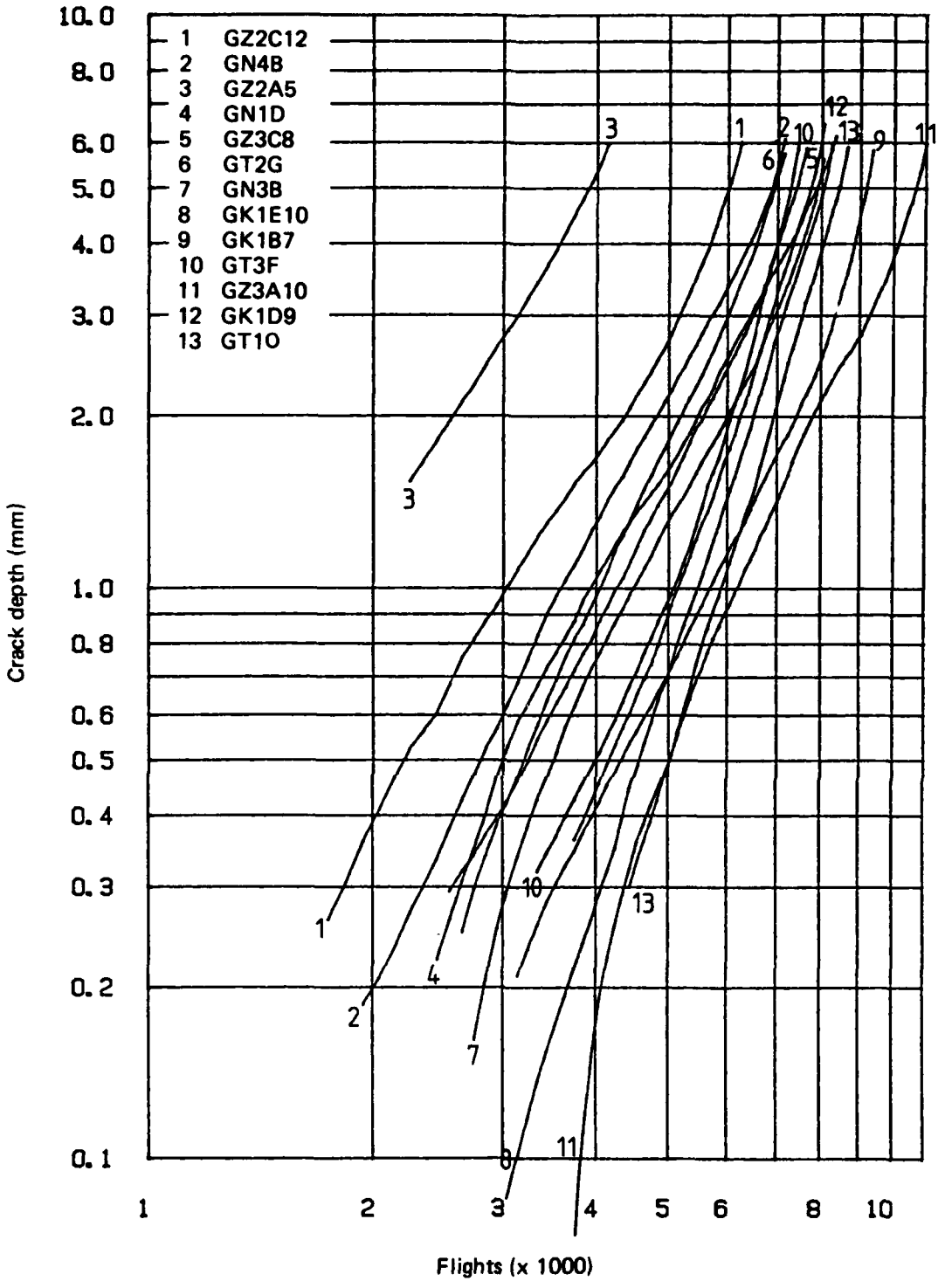

FIG. 9(d) FATIGUE CRACK GROWTH FROM 8 mm BOLT HOLE --
SPECIMENS WITH 0.125 INCH SLAN RIVETS, SPECTRUM TYPE I

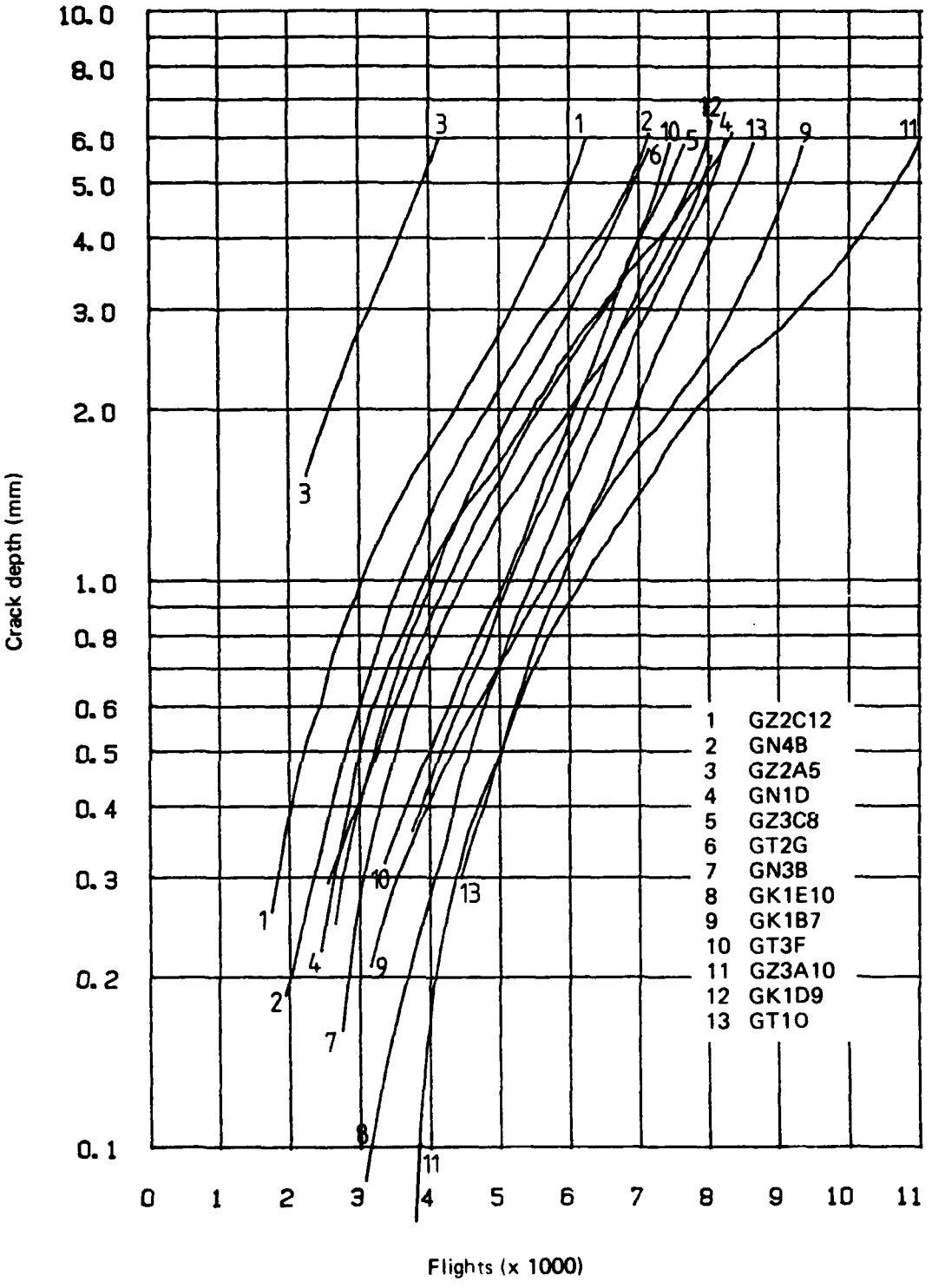

FIG. 9(c) FATIGUE CRACK GROWTH FROM 8 mm BOLT HOLE – SPECIMENS WITH 0.125 INCH SLAN RIVETS, SPECTRUM TYPE I

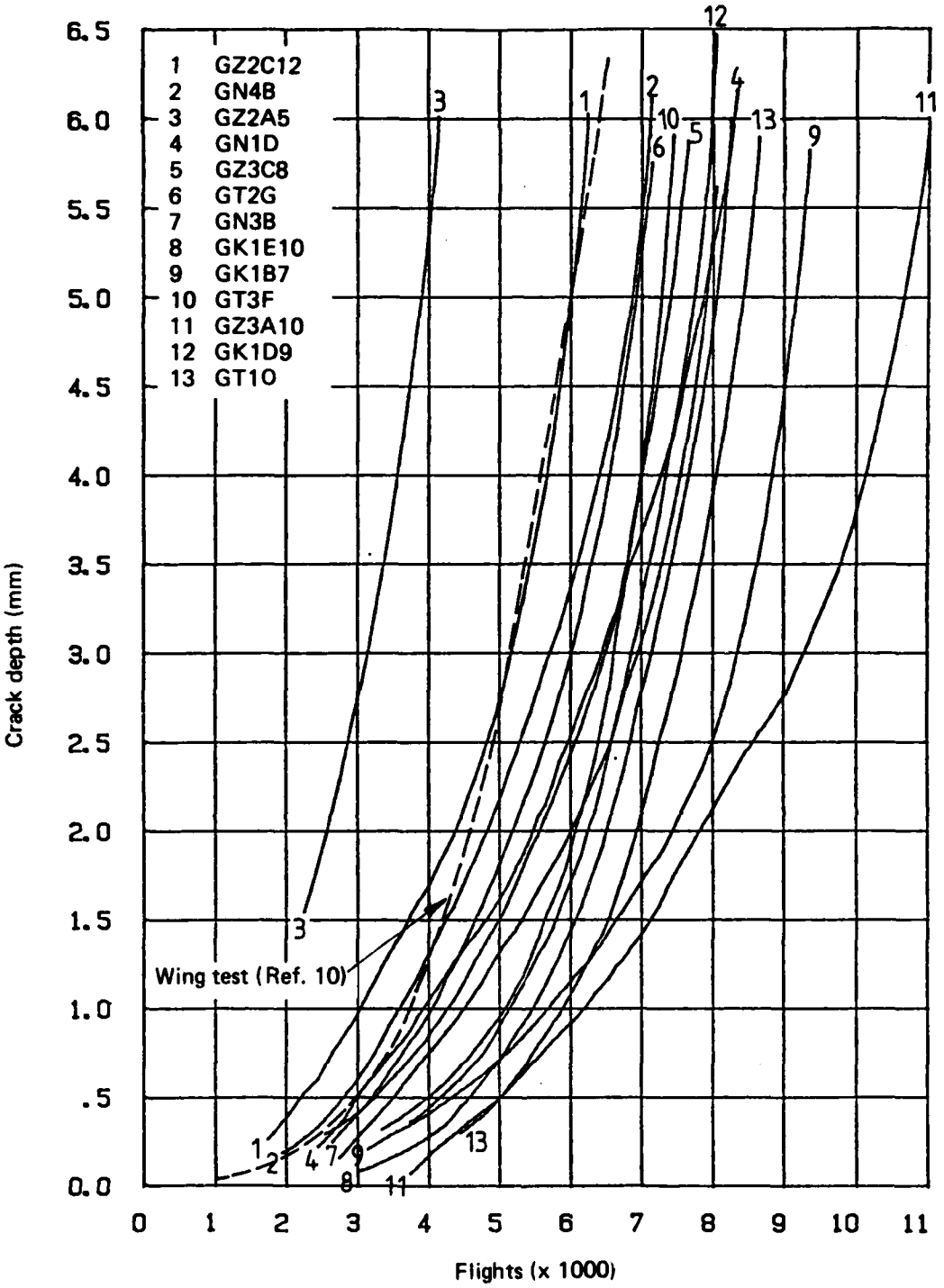

FIG. 9(b) FATIGUE CRACK GROWTH FROM 8 mm BOLT HOLE –
SPECIMENS WITH 0.125 INCH SLAN RIVETS, SPECTRUM TYPE I

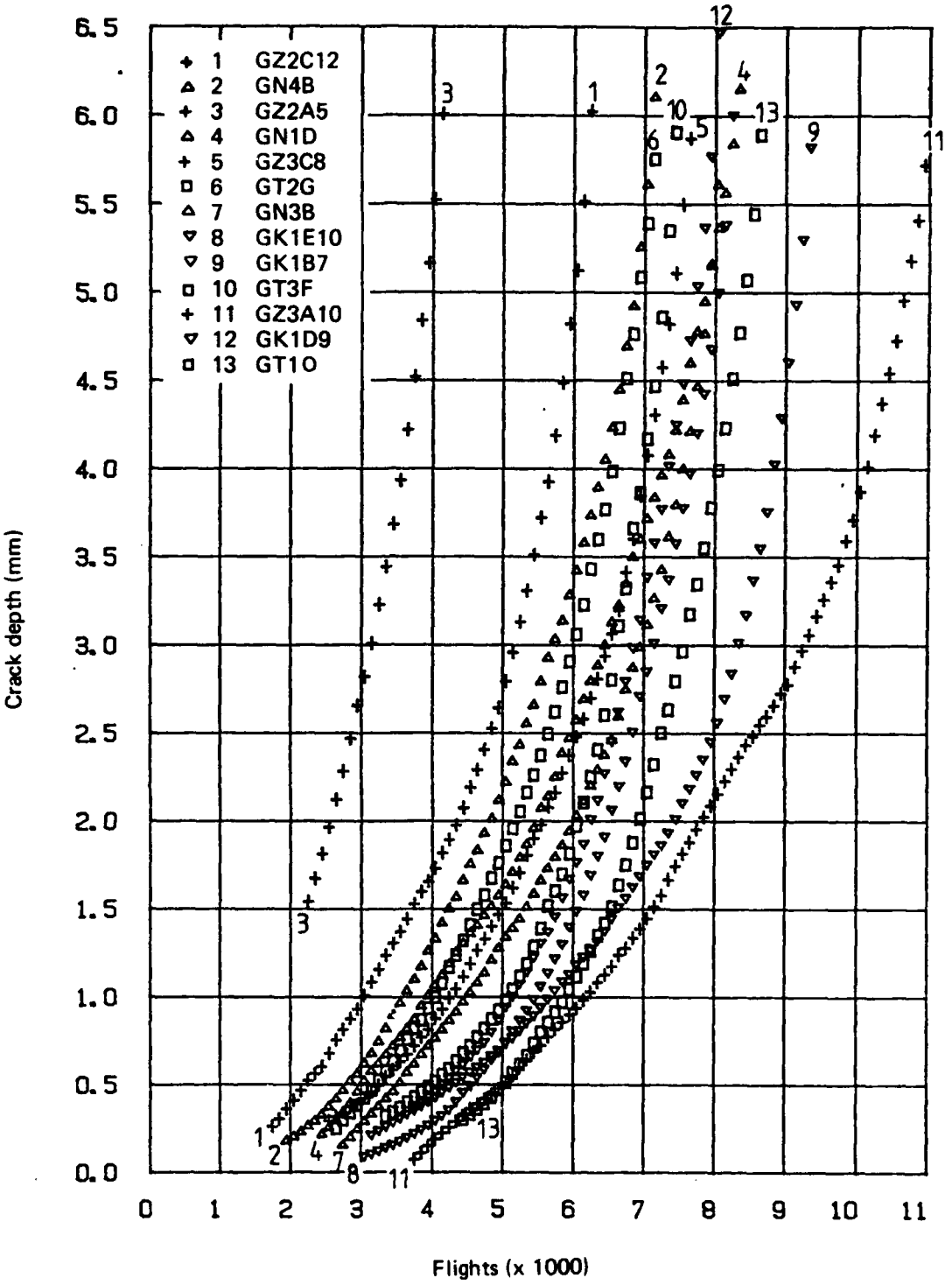

FIG. 9(a) FATIGUE CRACK GROWTH FROM 8 mm BOLT HOLE – SPECIMENS WITH 0.125 INCH SLAN RIVETS, SPECTRUM TYPE I

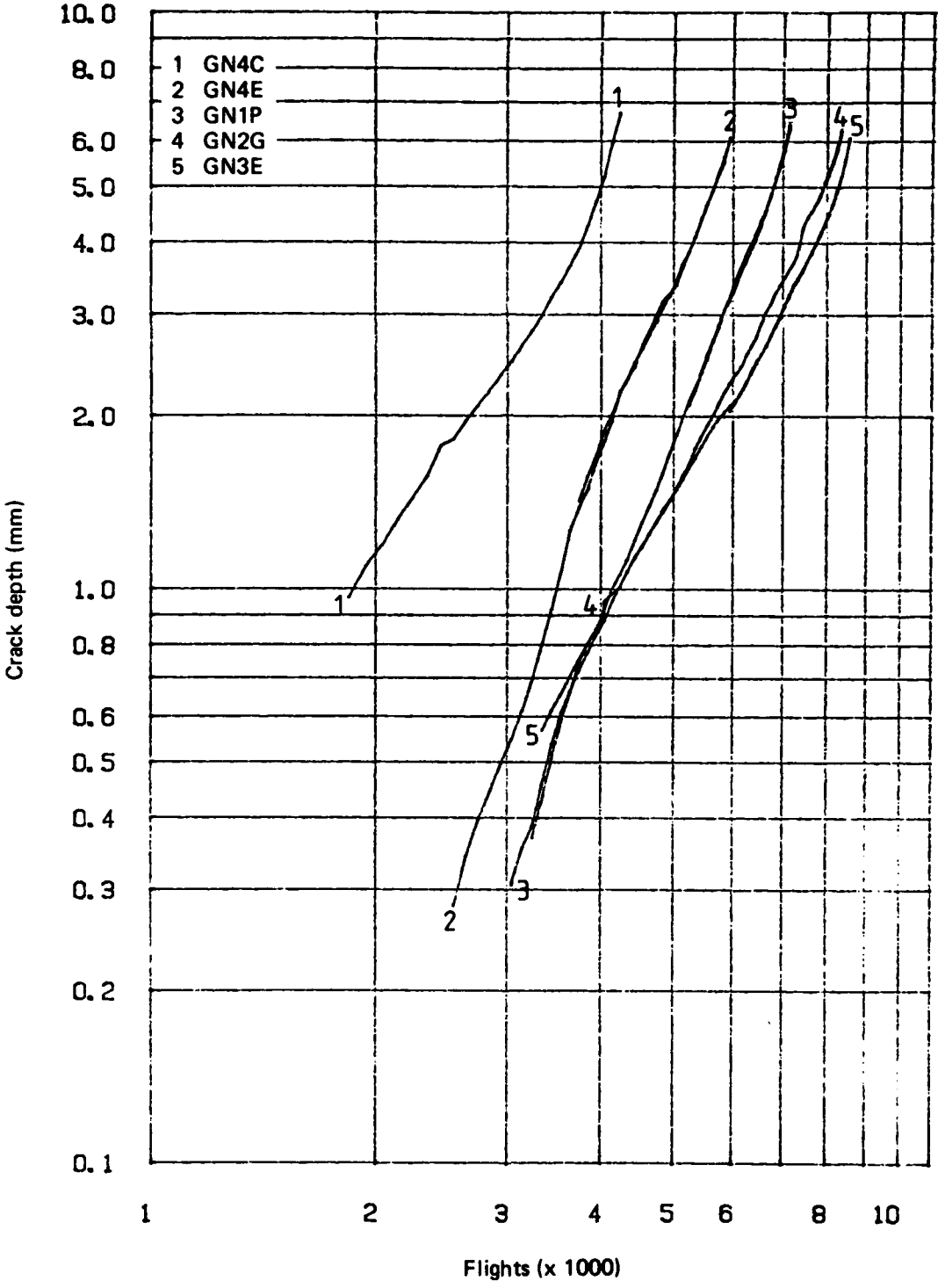

FIG. 8(c) FATIGUE CRACK GROWTH FROM 8 mm BOLT HOLE – SPECIMENS WITH 3.0 mm SLAN RIVETS

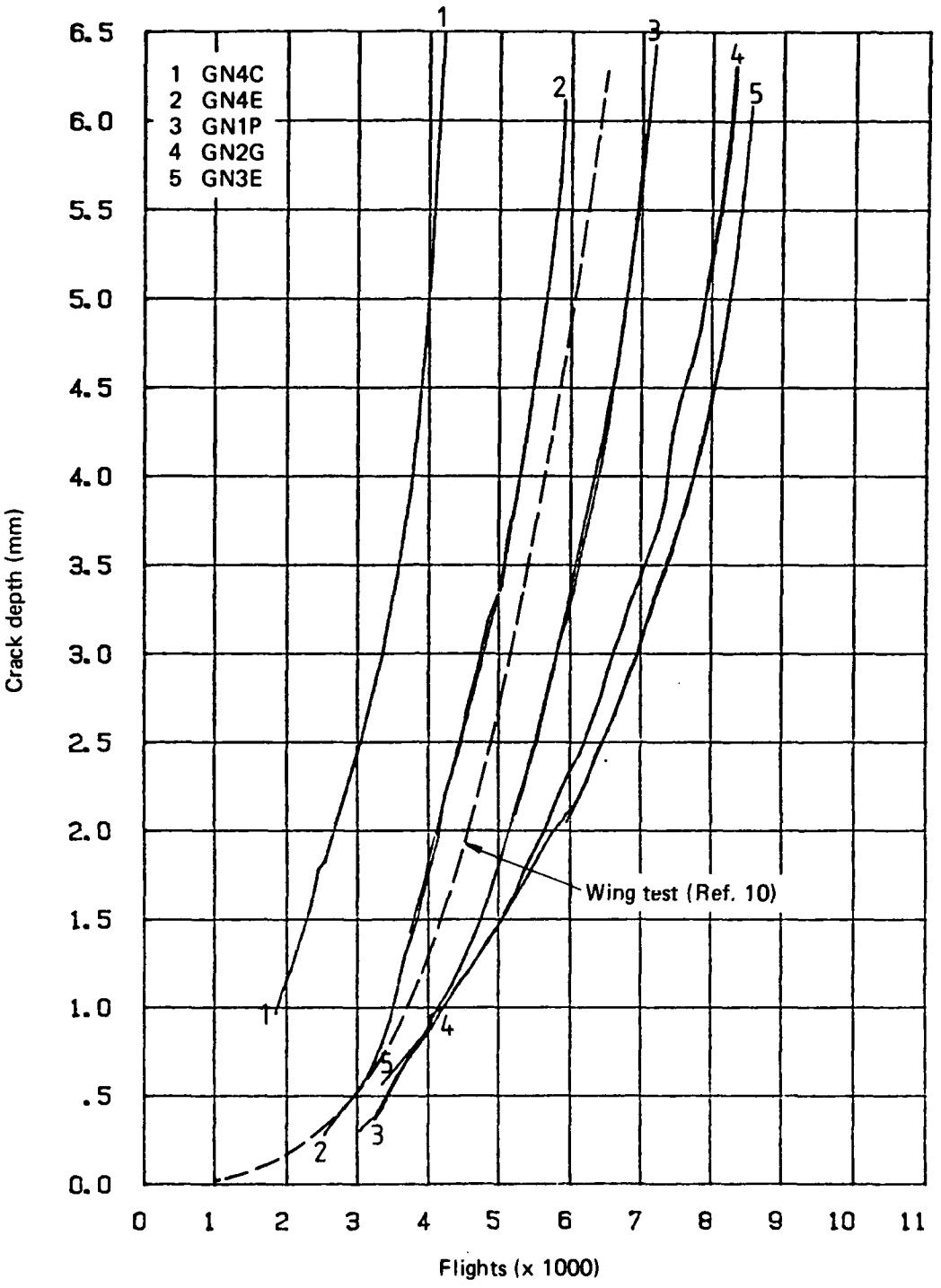

FIG. 8(b) FATIGUE CRACK GROWTH FROM 8 mm BOLT HOLE SPECIMENS WITH 3.0 mm SLAN RIVETS

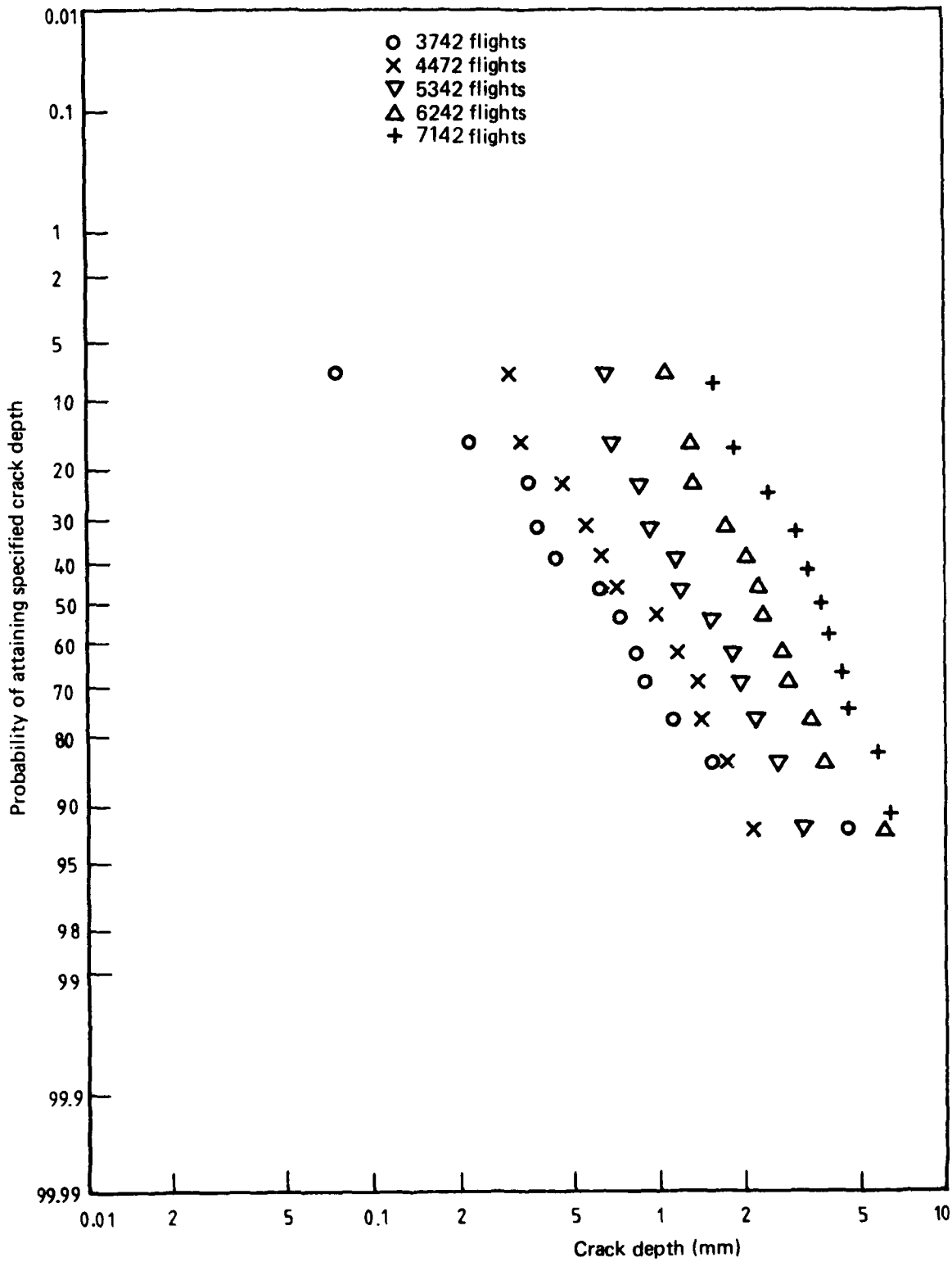

FIG. 12(b) PROBABILITY DISTRIBUTION OF CRACK DEPTHS AT DIFFERENT LIVES

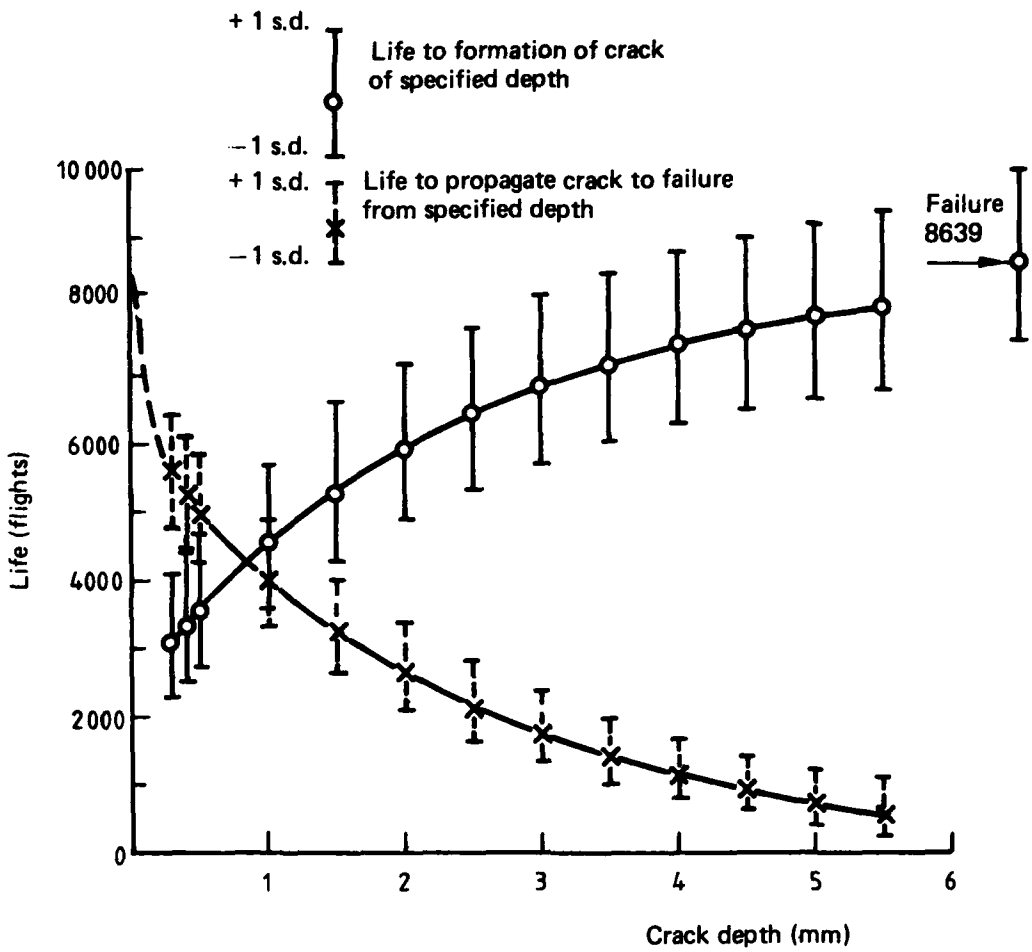

FIG. 13 LOG. AVERAGE LIVES TO AND FROM CRACKS OF SPECIFIED DEPTHS

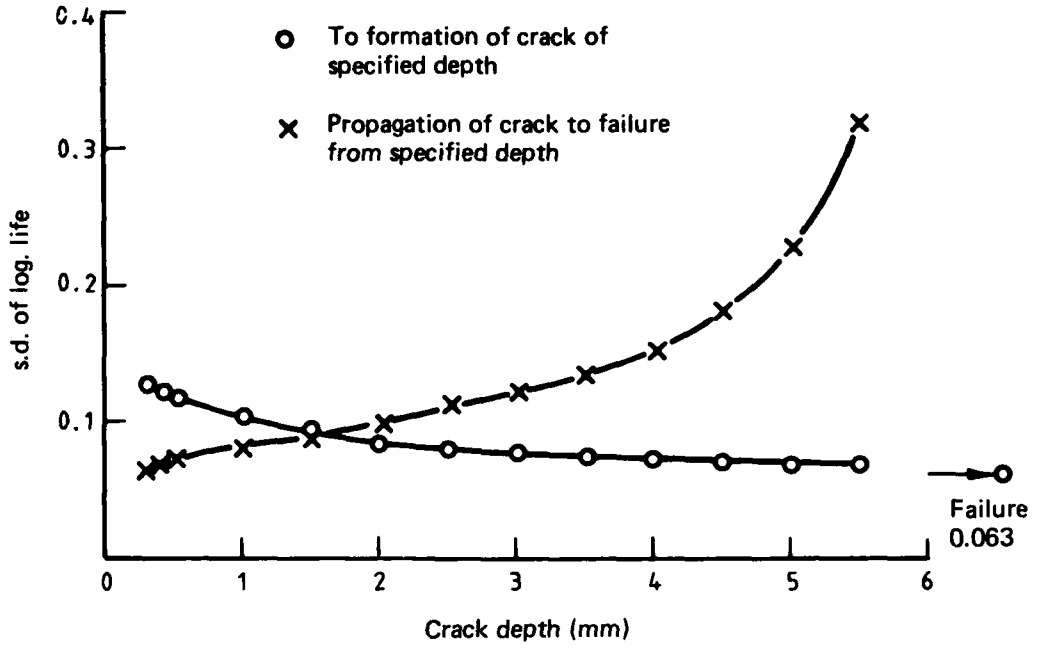

(a) s.d. of log. life

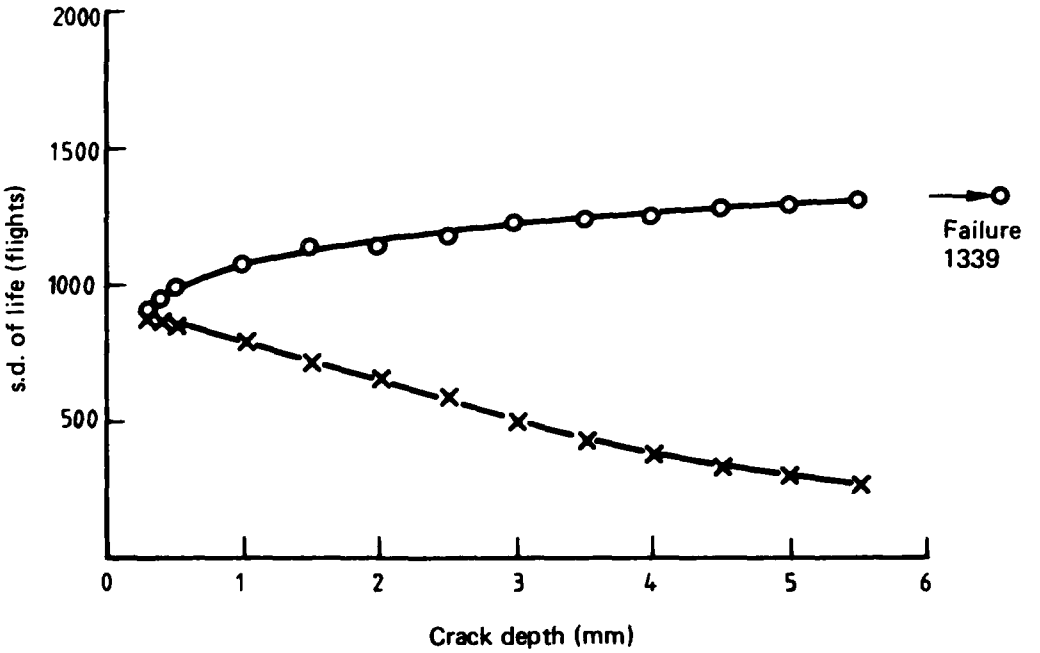

(b) Arithmetic s.d. of lives

FIG. 14 VARIABILITY IN LIVES TO FORMATION AND PROPAGATION OF CRACKS OF SPECIFIED DEPTHS

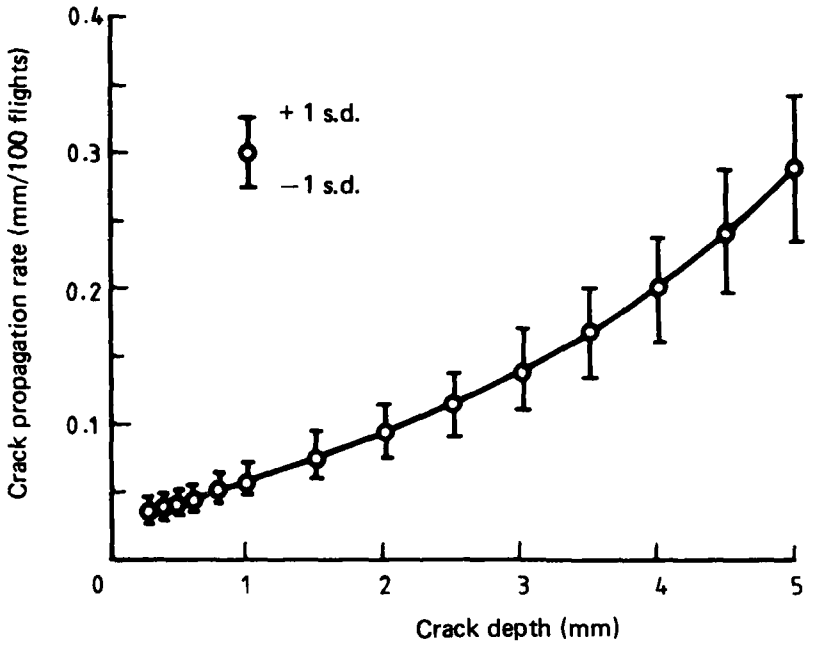

(a) Crack propagation rates

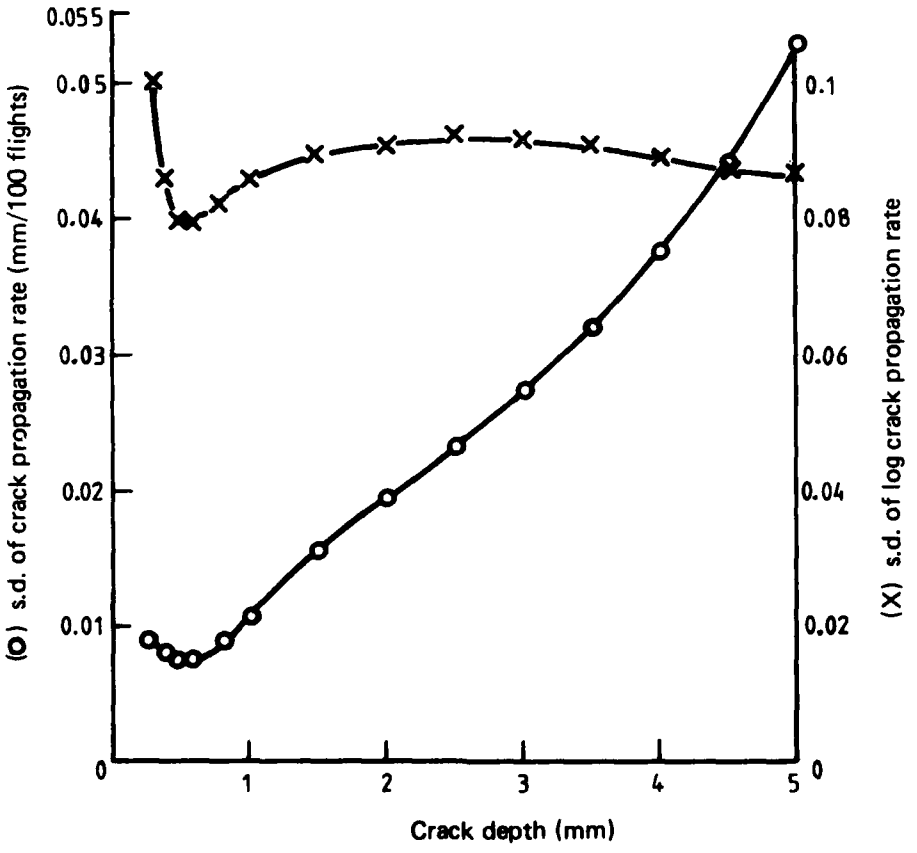

(b) s.d. of crack propagation rates

FIG. 15 RELATIONSHIPS BETWEEN CRACK PROPAGATION RATES AND CRACK DEPTHS

DISTRIBUTION

AUSTRALIA

DEPARTMENT OF DEFENCE

Central Office

Chief Defence Scientist
Deputy Chief Defence Scientist
Superintendent, Science and Program Analysis
Controller, External Relations, Projects and Analytical Studies } (1 copy)
Defence Science Adviser (U.K.) (Doc. Data sheet only)
Counsellor, Defence Science (U.S.A.) (Doc. Data sheet only)
Defence Science Representative (Bangkok)
Defence Central Library
Document Exchange Centre, D.I.S.B. (18 copies)
Joint Intelligence Organisation
Librarian H Block, Victoria Barracks, Melbourne
Director General—Army Development (NSO) (4 copies)

Aeronautical Research Laboratories

Director
Library
Superintendent—Structures
Superintendent—Materials
Divisional File—Structures
Authors: J. Y. Mann
R. A. Pell
A. S. Machin
D. G. Ford
G. S. Jost
G. W. Revill
B. C. Hoskin
J. M. Finney
L. M. Bland
C. K. Rider
J. M. Grandage
C. A. Patching
N. T. Goldsmith

Materials Research Laboratories

Director/Library

Defence Research Centre

Library

Navy Office

Navy Scientific Adviser
Directorate of Naval Aircraft Engineering

Army Office

Army Scientific Adviser
Engineering Development Establishment, Library

Air Force Office

Air Force Scientific Adviser
Director General Aircraft Engineering—Air Force
HQ Support Command (SLENGO)
Air Attache Paris (Sent direct from ARL)

DEPARTMENT OF DEFENCE SUPPORT

Government Aircraft Factories

Manager
Library

DEPARTMENT OF AVIATION

Library
Flying Operations and Airworthiness Division
Melbourne, Mr K. R. A. O'Brien
Canberra, Mr C. Torkington

STATUTORY AND STATE AUTHORITIES AND INDUSTRY

Australian Atomic Energy Commission, Director
CSIRO
Materials Science Division, Library
Trans-Australia Airlines, Library
Qantas Airways Limited
SEC of Vic., Herman Research Laboratory, Library
Ansett Airlines of Australia, Library
B.H.P., Melbourne Research Laboratories
Commonwealth Aircraft Corporation
Library
Mr K. J. Kennedy (Manager Aircraft Factory No. 1)
Manager, Design Engineering
Hawker de Havilland Aust. Pty. Ltd., Bankstown, Library

UNIVERSITIES AND COLLEGES

Adelaide	Barr Smith Library
Melbourne	Engineering Library
Monash	Hargrave Library Professor I. J. Polmear, Materials Engineering
Newcastle	Library
New England	Library
Sydney	Engineering Library
N.S.W.	Metallurgy Library
Queensland	Library
Tasmania	Engineering Library
Western Australia	Library
R.M.I.T.	Library

CANADA

CAARC Coordinator Structures
International Civil Aviation Organization, Library
Energy Mines and Resources Dept.
  Physics and Metallurgy Research Laboratories
NRC
  Aeronautical and Mechanical Engineering Library
  Division of Mechanical Engineering, Director

Universities and Colleges

Toronto	Institute for Aerospace Studies

FRANCE

ONERA, Library
AMD-BA
  Mr M. Peyrony
  Mr D. Chaumette

INDIA

CAARC Coordinator Structures
Defence Ministry, Aero Development Establishment, Library
Hindustan Aeronautics Ltd., Library
National Aeronautical Laboratory, Information Centre

INTERNATIONAL COMMITTEE ON AERONAUTICAL FATIGUE

Per Australian ICAF Representative (25 copies)

ISRAEL

Israel Air Force
Israel Aircraft Industries
Technion-Israel Institute of Technology
Professor J. Singer
Professor A. Buch

JAPAN

National Research Institute for Metals, Fatigue Testing Division
Institute of Space and Astronautical Science, Library

Universities

Kagawa University Professor H. Ishikawa

NETHERLANDS

National Aerospace Laboratory (NLR), Library

Universities

Technological University
of Delft Professor J. Schijve

NEW ZEALAND

Defence Scientific Establishment, Library
RNZAF, Vice Consul (Defence Liason)

Universities

Canterbury	Library Professor D. Stevenson, Mechanical Engineering

SWEDEN

Aeronautical Research Institute, Library
Swedish National Defense Research Institute (FOA), Library

SWITZERLAND

Armament Technology and Procurement Group
F+W (Swiss Federal Aircraft Factory)
  Mr L. Girard
  Dr H. Boesch
  Mr A. Jordi

UNITED KINGDOM

Ministry of Defence, Research, Materials and Collaboration
CAARC, Secretary (NPL)
Royal Aircraft Establishment
  Bedford, Library
  Farnborough, Library
Commonwealth Air Transport Council Secretariat
Admiralty Marine Technology Establishment, Library
National Gas Turbine Establishment
  Director, Pyestock North
National Physical Laboratory, Library
National Engineering Laboratory, Library
British Library, Lending Division
CAARC Coordinator, Structures
Fulmer Research Institute Ltd., Research Director
Motor Industry Research Association, Director
Rolls-Royce Ltd.
  Aero Division Bristol, Library
Welding Institute, Library
British Aerospace
  Hatfield-Chester Division, Library
British Hovercraft Corporation Ltd., Library
Short Brothers Ltd., Technical Library

Universities and Colleges

Bristol	Engineering Library
Nottingham	Science Library
Southampton	Library
Strathclyde	Library
Cranfield Institute of Technology	Library
Imperial College	Aeronautics Library

UNITED STATES OF AMERICA

NASA Scientific and Technical Information Facility
Applied Mechanics Reviews
Metals Information
The John Crerar Library
The Chemical Abstracts Service
Boeing Co.
  Mr R. Watson
  Mr J. C. McMillan
Lockheed-California Company
Lockheed Georgia
McDonnell Aircraft Company, Library
Nondestructive Testing Information Analysis Center
Fatigue Technology Inc., Mr R. L. Champoux

Universities and Colleges

Iowa	Professor R. I. Stephens
Illinois	Professor D. C. Drucker
Massachusetts Institute of Tech.	M.I.T. Libraries

SPARES (15 copies)

TOTAL (194 copies)

Department of Defence

DOCUMENT CONTROL DATA

1. a. AR No.	1. b. Establishment No.	2. Document Date	3. Task No.
AR-003-937	ARL-STRUC-R-405	July, 1984	DST 79/130

4. Title	5. Security	6. No. Pages
FATIGUE CRACK PROPAGATION IN MIRAGE IIIO WING MAIN SPAR SPECIMENS AND THE EFFECTS OF SPECTRUM TRUNCATION ON LIFE	a. document: Unclassified b. title: U c. abstract: U	27 7. No. Refs: 13

8. Author(s)	9. Downgrading Instructions
J. Y. Mann, R. A. Pell and A. S. Machin	

10. Corporate Author and Address	11. Authority (as appropriate)
Aeronautical Research Laboratories P.O. Box 4331, MELBOURNE, Vic., 3001	a. Sponsor c. Downgrading b. Security d. Approval —

12. Secondary Distribution (*of this document*)

Approved for public release

Overseas enquirers outside stated limitations should be referred through ASDIS, Defence Information Services Branch, Department of Defence, Campbell Park, CANBERRA, ACT, 2601.

13. a. This document may be ANNOUNCED in catalogues and awareness services available to . . .

No limitations

13. b. Citation for other purposes (*i.e. casual announcement*) may be (select) unrestricted (or) as for 13 a.

14. Descriptors		15. COSATI Group
Fatigue (materials)	Crack propagation	11130
Bolted joints	Load spectra	01030
Aircraft structures	Statistical analysis	
Aluminium alloys	Variability	

16. Abstract

As part of an investigation into the life extension and safe operation of the wings of the Mirage IIIO aircraft, a fatigue testing program and extensive fractographic examination was undertaken on specimens representing the critical section of the spar to assess the effects of truncating the maximum positive loads of the spectrum and provide information relating to fatigue crack propagation rates.

Under the fighter-type load spectrum adopted, truncation of the maximum load from +7·5 g to +6·5 g or to +5 g did not result in an increase in fatigue life, presumably because of the loss of the crack retardation potential of this rarely occurring high positive load.

A good linear relationship was found between the log. life and log. crack depth for individual specimens. At the smallest crack depth used for analysis (0·3 mm) no significant differences were found between the standard deviations of log. life to crack "initiation", for propagation or to final failure, nor in the corresponding standard deviations of arithmetic lives.

This page is to be used to record information which is required by the Establishment for its own use but which will not be added to the DISTIS data base unless specifically requested.

16. Abstract (Contd)

In considering the more general question of whether the greater contribution to variability in total life comes from that in "initiation" life or that in "propagation" life, cognizance must be taken of the analytical basis of the assessment—whether arithmetic or logarithmic. On a logarithmic basis the standard deviation of life to the formation of a crack of specific depth decreases with increasing crack depth, whereas on the arithmetic basis it increases. The converse applies in each case for the variability in propagation lives. On an arithmetic basis the standard deviation of the crack propagation rate increases with crack depth, that at a depth of 5 mm being about 7 times that at a depth of 0·5 mm. However the standard deviation of log. crack propagation rate is substantially constant irrespective of crack depth.

These findings are of significance in the numerical implementation of safe-life, durability and damage tolerance fatigue philosophies.

17. Imprint

Aeronautical Research Laboratories, Melbourne

18. Document Series and Number	19. Cost Code	20. Type of Report and Period Covered
Structures Report 405	251020	—

21. Computer Programs Used

—

22. Establishment File Ref(s)

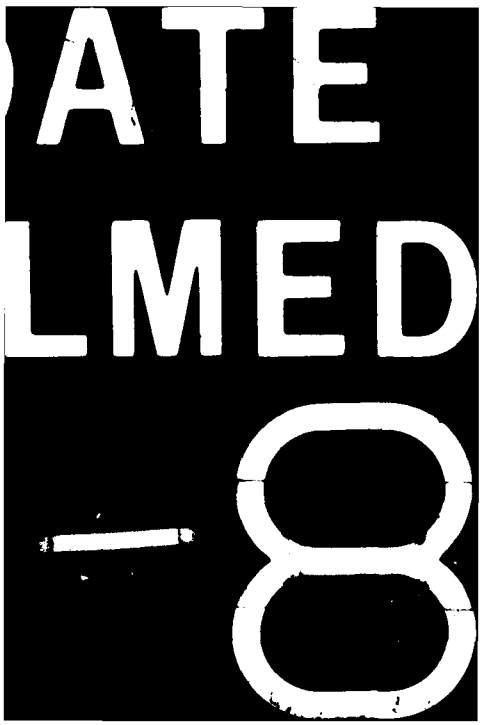
ATE
LMED
8